Reduction in sound discrimination in noise is related to envelope similarity and not to a decrease in envelope tracking abilities

Samira Souffi, Léo Varnet, Meryem Zaidi, Brice Bathellier, Chloé Huetz, Jean-Marc Edeline

Reduction in sound discrimination in noise is related to envelope similarity and not to a decrease in envelope tracking abilities

Samira Souffi[1, §], Léo Varnet[2], Meryem Zaidi[1], Brice Bathellier[3], Chloé Huetz[1] and Jean-Marc Edeline*[1]

[1] Paris-Saclay Institute of Neuroscience (Neuro-PSI, UMR 9197), CNRS - Université Paris-Saclay, Centre CEA Saclay - Bât 151, 91400 Saclay, France.
[2] Laboratoire des systèmes perceptifs, UMR CNRS 8248, Département d'Etudes Cognitives, Ecole Normale Supérieure, Université Paris Sciences & Lettres, Paris, France.
[3] Institut de l'Audition, Institut Pasteur, Université de Paris, INSERM, Paris F-75012, France.

Number of pages: 33
Number of figures: 7
Number of words in abstract: 166
Number of words in introduction: 994
Number of words in discussion: 2429

Running title: Envelope tracking of noisy sounds in the auditory system

* *Corresponding Author:*
Jean-Marc Edeline
UMR 9197, Neuro-PSI (Institut des Neurosciences Paris-Saclay)
CNRS - Université Paris-Saclay,
Centre CEA Saclay, Bâtiment 151
91400 Saclay cedex, France
email: jean-marc.edeline@universite-paris-saclay.fr

§ current address: Edmond and Lily Safra Center for Brain Sciences, The Hebrew University of Jerusalem, Edmond J. Safra Campus, Givat Ram, Jerusalem 9190401, Israel.

First author profile

Samira Souffi completed her PhD in France at the Institute of Neuroscience in Paris-Saclay University (NeuroPSI) under the supervision of Dr. Jean-Marc Edeline. Her research was focused on understanding the effects of background noises on the neuronal discrimination in the whole auditory system. Her postdoctoral research in Prof. Israel Nelken laboratory (ELSC, Hebrew University of Jerusalem, Israel) describes the neuronal networks involved in developing sound preferences (e.g. music preferences) on mice by recording the calcium activity in both the reward and the auditory systems.

Key points:

* In quiet, envelope tracking in the low amplitude modulation range (<20 Hz) is correlated with the neuronal discrimination between communication sounds as quantified by mutual information from the cochlear nucleus up to the auditory cortex.
* At each level of the auditory system, auditory neurons keep their abilities to track the communication sound envelopes in situations of acoustic degradation such as vocoding and the addition of masking noises up to a signal-to-noise ratio of -10 dB.
* In noise, the increase in between-stimulus envelope similarity explains both the reduction in behavioral and neuronal discrimination in the auditory system.
* Envelope tracking can be viewed as a universal mechanism allowing neural and behavioral discrimination as long as the temporal envelope of communication sounds display some differences.

Abstract

Humans and animals constantly face challenging acoustic environments such as various background noises that impair the detection, discrimination and identification of behaviorally relevant sounds. Here, we disentangled the role of temporal envelope tracking on the reduction in neuronal and behavioral discrimination between communication sounds in situations of acoustic degradations. By collecting neuronal activity from six different levels of the auditory system, from auditory nerve up to secondary auditory cortex in anesthetized guinea-pigs, we found that tracking of slow changes of the temporal envelope is a general functional property of auditory neurons for encoding communication sounds in quiet and also in adverse, challenging, conditions. Results from a Go/No-Go sound discrimination task on mice support the idea that the loss of distinct slow envelope cues in noisy conditions impacted the discrimination performance. Together, these results suggest that envelope tracking is potentially a universal mechanism operating in the central auditory system, which allows the detection of any between-stimuli difference in slow envelope and thus cope with degraded conditions.

Keywords: Auditory system; Temporal envelope tracking; Neuronal and behavioral discrimination; Degraded acoustic conditions.

Abbreviation list

ABR: auditory brainstem responses

A1: primary auditory cortex

AM: amplitude modulation

CN: cochlear nucleus

CNIC: central nucleus of inferior colliculus

E: envelope

ERB: equivalent rectangular bandwidth

FM: frequency modulation

H: high

L: low

M: middle

MGv: ventral part of medial geniculate body

MI: mutual information

MUA: multiunit activity

PSTH: peristimulus histogram

R: correlation coefficient

$Rmax_{E\text{-}PSTH}$: maximal value of correlation coefficient between envelope and PSTH

R_{Random}: correlation coefficient between envelope and shuffled PSTH

RMS: root mean square

sANF: simulated auditory nerve fibers

SNR: signal-to-noise ratio

SR: spontaneous rate

TFRP: time-frequency response profile

VRB: ventral-rostral belt (secondary auditory cortex)

Introduction

In humans, speech signals are characterized by rhythmic streams of amplitude and frequency modulations (AM and FM) that convey phoneme, syllable, word, and phrase information (Rosen 1992, Varnet et al., 2017, Ding et al., 2017). It is known for several decades that the low-frequency modulations of the temporal envelope carry essential cues for speech perception (Drullman et al., 1994a,b; Shannon et al., 1995; Zeng et al., 2005): even in challenging conditions (including in various types of noise), the human auditory system has the capacity to process highly degraded speech as long as the temporal envelope modulations below 20 Hz are preserved (Drullman et al., 1994a, b; Shannon et al., 1995; Zeng et al., 2005). This is consistent with electroencephalographic (EEG) and magnetoencephalographic (MEG) studies in which cortical responses were found in phase with the temporal envelope of speech signals and strongly correlated with the average level of speech comprehension both for normal and compressed speech (Ahissar et al., 2001; Luo and Poeppel, 2007; Ding et al., 2014). In a recent study, Ortiz-Barajas and colleagues (2021) have found that newborns possess the neural capacity to track the amplitude and the phase of the speech envelope in their native language (French), as well as in rhythmically similar and different unfamiliar languages (Spanish and English). These results support the hypothesis that speech envelope tracking may be a necessary prerequisite, although not sufficient, for speech comprehension (Kösem et al., 2016, 2017).

In animals, the synchronization of auditory cortex responses with the temporal envelope of guinea pig vocalizations has been observed in several studies (Wallace et al., 2005; Wallace & Palmer, 2009; Grimsley et al., 2011, 2012), some of them even suggesting that cortical responses could be isomorphic to the vocalization envelope (Figure 2A in Grimsley et al., 2012). Using speech stimuli with different levels of degradation (clear, conversational and compressed), Abrams and colleagues (2017) recorded responses of auditory cortex neurons in guinea pigs and showed that populations of cortical neurons encode both the periodicity and the temporal broadband envelope of the speech signal. These temporal representations in auditory cortex were quite resistant to the degradations (conversational and compressed speech) and additional studies have pointed out that cortical neurons can still respond to target stimuli in important levels of noise (between -5 and 0 dB SNR, Nagarayan et al., 2002; Narayan et al., 2007; Shetake et al., 2011; Homma et al., 2020). At the subcortical level, several studies revealed in both mammals and birds that the average responses of inferior colliculus neurons can reflect the communication sound envelope (Suta et al., 2003; Woolley et al., 2006; Rode et al., 2013).

Here, we used acoustic degradations that differentially affected the similarities between acoustic envelopes: vocoders strongly altered the spectral cues but preserved most of the temporal

information whereas noise addition produced spectrotemporal degradations, reduced the temporal cues while introducing irrelevant envelope fluctuations and altered the spectral cues (Fig. 1 of Souffi et al., 2020). We used a stationary noise which strongly increased the acoustic similarity between the envelopes and a chorus noise which differed between the four envelopes and therefore masked the vocalizations while not inducing an increase in the overall similarity of the stimuli. We previously showed that the addition of a stationary noise strongly impaired the neuronal discrimination performance at the subcortical and cortical levels, whereas it was less impaired in the vocoding conditions (Fig. 6-9 of Souffi et al., 2020). To go further, our main goal in the current study was to determine whether the similarities between acoustic envelopes or the loss in envelope tracking ability by auditory neurons reduce or even prevent the neuronal and behavioral discrimination in situations of acoustic degradations. In a condition-independent scenario, the neurons keep the same intrinsic ability to track the stimulus envelopes whatever the acoustic conditions (in quiet and in degraded conditions): As long as the stimulus envelopes differ, the neurons will discriminate the stimuli. In contrast, in a condition-dependent scenario, the acoustic degradations reduce the neurons' ability to track the stimulus envelopes. This deleterious effect can potentially occur when the neurons are strongly driven by the acoustic degradations (such as noise addition) leading to limited dynamic ranges for coding the target stimuli. This occurs for example for the responses of auditory nerve fibers (ANF) to tones in continuous noise. Even if the responses to 120-300Hz periodic AM stimuli were still preserved at 0 and +6 dB SNR (Figure 6 of Frisina et al., 1996), many studies reported that the rate-level functions of ANF tested with pure tones were largely altered in noise: in many cases the responses did not reach the same saturation level (Rhode et al., 1978; Geisler and Sinex, 1980; Costalupes et al., 1984; Frisina et al., 1996) or the whole curve was shifted toward the right (Rhode et al., 1978; Costalupes et al., 1984) indicating that the thresholds were higher and the dynamic ranges were smaller than in quiet. This was also a function of the bandwidth of the noise and the types of ANF (i.e., the effects differed between low, medium or high spontaneous rate fibers, see for example Reiss et al., 2011). Based on these studies, it seems that, as early as the auditory nerve, the detection of AM cues contained in target stimuli, and therefore the tracking abilities of central auditory neurons, can be reduced. Similar results have been observed in the inferior colliculus (Ramachandran et al., 2000).

In an attempt to dissociate between these two scenarios, we evaluated the relationship between the envelope tracking of sounds and the neuronal discrimination in the entire auditory system. We simulated auditory nerve fiber (sANF) responses (with a widely-used model, Bruce et al., 2018) and recorded the neuronal activity in five auditory structures in response to four conspecific vocalizations presented in quiet, using three tone-vocoders and two types of noise (a stationary and a chorus noise at three SNRs +10, 0 and -10 dB) in anesthetized guinea pigs. We found that

subcortical and cortical neurons track the envelopes in the low AM range (<20Hz), with a high degree of fidelity in original and degraded conditions, suggesting that the auditory system maintains a robust temporal representation from the auditory nerve to the auditory cortex. Behaving mice were also able to discriminate between these communication sounds, and performed the task above chance level in all noisy conditions. Overall, our results demonstrate that the between-stimulus envelope similarity, which increases in noise, negatively correlates both with the neuronal discrimination and the behavioral performance.

Materials and Methods

Most of the Methods are similar to those described in Souffi and colleagues (2020).

Subjects for the electrophysiological and behavioral experiments

These experiments were performed under the national license A-91-557 (project 2014-25, authorization 05202.02) and using the procedures N° 32-2011 and 34-2012 validated by the Ethic committee N°59 (CEEA, (Comité d'Ethique pour l'Expérimentation Animale) Paris Centre et Sud). All surgical procedures were performed in accordance with the guidelines established by the European Communities Council Directive (2010/63/EU Council Directive Decree).

Extracellular recordings were obtained from 47 adult pigmented guinea pigs (aged 3 to 16 months old, 36 males, 11 females) at five different levels of the auditory system: the cochlear nucleus (CN), the inferior colliculus (IC), the medial geniculate body (MGB), the primary (A1) and secondary auditory cortex (area VRB). Animals, weighing from 515 to 1100 g (mean 856 g), came from our own colony housed in a humidity (50-55%) and temperature (22-24°C)-controlled facility on a 12 h/12 h light/dark cycle (light on at 7:30 A.M.) with free access to food and water.

Two days before the electrophysiological experiment the animal's pure-tone audiogram was determined by testing auditory brainstem responses (ABR) under isoflurane anesthesia (2.5%) as described in Gourévitch and colleagues (2009). A software (RTLab, Echodia, Clermont-Ferrand, France) allowed averaging 500 responses during the presentation of each pure-tone frequency and each intensity (between 0.5 and 32 kHz, duration: 10 ms, rise-fall time: 2 ms) delivered by a speaker (Knowles Electronics) placed in the animal's right ear canal. The threshold of each ABR was defined as the lowest intensity where a small ABR wave could still be detected (usually wave III). For each frequency, the threshold was determined by gradually decreasing the sound intensity (from 80 dB down to -10 dB SPL). There was a perfect agreement between the thresholds visually determined by two co-authors (SS, JME). Based upon a large database of more than 250 guinea pigs, we considered that all animals used in this study had normal pure-tone audiograms (Gourévitch et al., 2009; Gourévitch and Edeline, 2011).

Behavioral experiments were performed on nine eight-weeks old C57Bl/6J female mice (see *Behavioral Go/No-Go discrimination task* part for more details).

Acoustic stimuli

The acoustic stimuli were the same as in Souffi and colleagues (2020, 2021). They were generated using MatLab, transferred to a RP2.1-based sound delivery system (TDT) and sent to a Fostex speaker (FE87E). The speaker was placed at 2 cm from the guinea pig's right ear, a distance at

which the speaker produced a flat spectrum (± 3 dB) between 140 Hz and 36 kHz. Calibration of the speaker was made using noise and pure tones recorded by a Bruel and Kjaer microphone 4133 coupled to a preamplifier BandK 2169 and a digital recorder Marantz PMD671.

Time-Frequency Response Profiles (TFRP) were determined using 129 pure-tone frequencies covering eight octaves (0.14-36 kHz) and presented at 75 dB SPL. The tones had a gamma envelope given by $\gamma(t) = (\frac{t}{4})^2 e^{\frac{-t}{4}}$, where t is time in ms. At a given stimulus level, each frequency was repeated eight times at a rate of 2.35 Hz in pseudorandom order. The duration of these tones over half-peak amplitude was 13.6 ms and at 50ms the sound intensity was 6.7 dB SPL. There was no overlap between tones.

A set of four conspecific vocalizations was used to assess the neuronal responses to communication sounds. These vocalizations were recorded from animals of our colony. Pairs of animals were placed in the acoustic chamber and their vocalizations were recorded by a Bruel & Kjaer microphone 4133 coupled to a preamplifier B&K 2169 and a digital recorder Marantz PMD671. A large set of whistle calls was loaded in the Audition software (Adobe Audition 3) and four representative examples of whistles were selected (Figure 1A, left panel). As shown in Figure 1B (left panel), their overall envelopes clearly differed, W2 and W4 envelopes being the closest from each other. The four whistles were presented in two frozen noises ranging from 10 to 24 000 Hz. To generate these noises, audio-recordings were performed in the colony room where a large group of guinea pigs were housed (30-40 animals; 2-4 animals/cage). Several 4-seconds of audio recordings were added up to generate the "chorus noise", whose power spectrum was computed using the Fourier transform. The chorus noise masking each target vocalization was slightly different in terms of spectro-temporal content. The chorus noise spectrum was then used to shape the spectrum of a Gaussian white noise. The resulting "vocalization-shaped stationary noise" therefore matched the "chorus-noise" audio spectrum. Figure 1B displays the overall envelopes of the four whistles in the vocalization-shaped stationary noise (third panel) and in the chorus noise (fourth panel) with signal-to-noise ratios (SNR) of +10, 0 and -10 dB.

The four selected whistles were also processed by three tone vocoders (Gnansia et al., 2009, 2010). In the following figures, the unprocessed whistles will be referred to as the original versions, and the vocoded versions as Voc38, Voc 20, and Voc10 using 38, 20, and 10 bands, respectively. In contrast to previous studies that used noise-excited vocoders (Nagarajan et al., 2002; Ranasinghe et al., 2012; Ter-Mikaelian et al., 2013), a tone vocoder was used here, because noise vocoders were found to introduce random (i.e., non-informative) intrinsic temporal-envelope fluctuations distorting the crucial spectro-temporal modulation features of communication sounds (Shamma and Lorenzi, 2013; Kates, 2011; Stone et al., 2011). Figure 1B displays the overall envelopes of the 38-band vocoded (first row, second panel), the 20-band vocoded (second row, second panel) and the

10-band vocoded (third row, second panel) versions of the four whistles. The three vocoders differed only in terms of the number of frequency bands (i.e., analysis filters) used to decompose the whistles (38, 20 or 10 bands). The 38-band vocoding process is briefly described below, but the same principles apply to the 20-band or the 10-band vocoders. Each digitized signal was passed through a bank of 38 fourth-order Gammatone filters (Patterson, 1987) with center frequencies uniformly spaced along a guinea-pig adapted ERB (Equivalent Rectangular Bandwidth) scale ranging from 50 to 35505 Hz (Sayles and Winter, 2010).

Overall envelope extraction

In each frequency band, the temporal envelope was extracted using full-wave rectification and low-pass filtering at 64 Hz with a zero-phase, sixth-order Butterworth filter. The resulting envelopes were used to amplitude modulate sine-wave carriers with frequencies at the center frequency of the Gammatone filters, and with random starting phase. Impulse responses were peak-aligned for the envelope (using a group delay of 16 ms) and the acoustic temporal fine structure across frequency channels (Hohmann, 2002). The modulated signals were finally weighted and summed over the 35 frequency bands (see section "*Quantification of the envelope tracking"*). The weighting compensated for imperfect superposition of the bands' impulse responses at the desired group delay. The weights were optimized numerically to achieve a flat frequency response.

Surgical procedures

All guinea pigs were anesthetized by an initial injection of urethane (1.2 g/kg, i.p.) supplemented by additional doses of urethane (0.5 g/kg, i.p.) when reflex movements were observed after pinching the hind paw (usually 2-4 times during the recording session). A single dose of atropine sulfate (0.06mg/kg, s.c.) was given to reduce bronchial secretions and a small dose of buprenorphine was administered (0.05mg/kg, s.c.) as urethane has no analgesic properties. After placing the animal in a stereotaxic frame, a craniotomy was performed and a local anesthetic (Xylocain 2%) was injected in the wound.

For auditory cortex recordings (area A1 and VRB), a craniotomy was performed above the left temporal cortex. The dura above the auditory cortex was removed under binocular control and the cerebrospinal fluid was drained through the cisterna to prevent the occurrence of oedema. For the recordings in MGB, a craniotomy was performed above the most posterior part of the MGB (8mm posterior to Bregma) to reach the left auditory thalamus at a location where the MGB is mainly composed of its ventral, tonotopic, part (Redies et al., 1989; Edeline et al., 1999; Anderson et al., 2007; Wallace et al., 2007). For IC recordings, a craniotomy was performed above the IC and portions of the cortex were aspirated to expose the surface of the left IC (Malmierca et al., 1995, 1996; Rees et al., 1997). For CN recordings, after opening the skull above the right cerebellum,

portions of the cerebellum were aspirated to expose the surface of the right CN (Paraouty et al., 2018).

After all surgeries, a pedestal in dental acrylic cement was built to allow an atraumatic fixation of the animal's head during the recording session. The stereotaxic frame supporting the animal was placed in a sound-attenuating chamber (IAC, model AC1). At the end of the recording session, a lethal dose of Exagon (pentobarbital >200 mg/kg, i.p.) was administered to the animal.

Recording procedures

Data from multi-unit recordings were collected in 5 auditory structures, the non-primary cortical area VRB, the primary cortical area A1, the medial geniculate body (MGB), the inferior colliculus (IC) and the cochlear nucleus (CN). In a given guinea pig, neuronal recordings were only collected in one auditory structure.

Cortical extracellular recordings were obtained from arrays of 16 tungsten electrodes (TDT, TuckerDavis Technologies; ø: 33 µm, <1 MΩ) composed of two rows of 8 electrodes separated by 1000 µm (350 µm between electrodes of the same row). A silver wire, used as ground, was inserted between the temporal bone and the dura mater on the contralateral side. The location of the primary auditory cortex was estimated based on the pattern of vasculature observed in previous studies (Wallace et al., 2000; Gaucher et al., 2013, 2020; Gaucher and Edeline, 2015). The non-primary cortical area VRB was located ventral to A1 and distinguished by its longer response latencies to pure tones (Rutkowski et al., 2002; Grimsley et al., 2012). For each experiment, the position of the electrode array was set in such a way that the two rows of eight electrodes sampled neurons responding from low to high frequency when progressing in the rostro-caudal direction [see examples in Figure 1 of Gaucher et al., (2012) and in Figure 6A of Occelli et al., (2016)].

In the MGB, IC and CN, the recordings were obtained using 16-channel multi-electrode arrays (NeuroNexus) composed of one shank (10 mm) of 16 electrodes spaced by 110 µm and with conductive site areas of 177µm^2. The electrodes were advanced vertically (for MGB and IC) or with a 40° angle to the CN surface until responses to pure tones could be detected on at least 10 electrodes.

All thalamic recordings were from the ventral part of MGB (see above surgical procedures) and all displayed response latencies < 9ms. At the collicular level, we distinguished the lemniscal and non-lemniscal divisions of IC based on depth and the latencies of pure tone responses. We excluded the most superficial recordings (until a depth of 1500µm) and those exhibiting latencies >= 20ms in an attempt to select recordings from the central nucleus of IC (CNIC). At the level of the cochlear nucleus, the recordings were collected from both the dorsal and ventral divisions.

The raw signal was amplified 10,000 times (TDT Medusa). It was then processed by an RX5 multichannel data acquisition system (TDT). The signal collected from each electrode (sampling rate 25kHz on each channel) was filtered (610-10000 Hz) to extract multi-unit activity (MUA). The trigger level was set for each electrode to select the largest action potentials from the signal with a 1ms precision. On-line and off-line examination of the waveforms suggests that the MUA collected here was made of action potentials generated by a few neurons at the vicinity of the electrode.
However, as we did not use tetrodes, the result of several clustering algorithms (Pouzat et al., 2002; Quiroga et al., 2004; Franke et al., 2015) based on spike waveform analyses were not reliable enough to isolate single units with good confidence. Although these are not direct proofs, the facts that the electrodes were of similar impedance (0.5-1 MOhm) and that the spike amplitudes had similar values (100-300 μV) for the cortical and the subcortical recordings were two indications suggesting that the cluster recordings obtained in each structure included a similar number of neurons. Even if a similar number of neurons were recorded in the different structures, we cannot discard the possibility that the homogeneity of the multi-unit recordings (in terms of number of cells contributing to each recording) differ between structures. By collecting several hundreds of recordings in each structure, these potential differences should be attenuated in the present study.

Simulations of auditory nerve fiber responses

A computational model of auditory nerve fiber responses was used to assess whether the envelope-tracking properties measured in the central auditory system could be a mere consequence of the processing taking place at peripheral levels. For this purpose, we used a well-established and widely-used model of the auditory periphery (Bruce et al., 2018). This model provides a phenomenological description of the major functional stages of the auditory periphery, from the middle ear up to the auditory nerve (Osses et al., 2022). The implementation used in the present study is available as the routine ‘bruce2018’ within the AMT toolbox (v1.0) for MATLAB (Majdak et al., 2022).
In order to make the simulated data as comparable as possible to the neuronal responses collected in the electrophysiological experiments, the distribution of cochlear center frequencies was chosen to be similar to the best frequencies obtained from the CN data. Default parameters were used for the later stages of the model. For each cochlear channel, five auditory-nerve fibers were simulated with different spontaneous rates (SR): 1 low-SR fiber (SR = 0.1 spikes/s), 1 medium-SR fiber (SR = 4 spikes/s) and 3 high-SR fibers (SR = 100 spikes/s). The outcome of the model corresponds to the aggregated responses of these 5 simulated auditory nerve fibers (sANF) in an attempt (i) to keep the physiological ratio between low, medium and high threshold fibers and (ii) to roughly match the

number of cells contributing to the MUA collected in the central auditory structures (<6 neurons at the vicinity of the electrode).

The responses to twenty repetitions of each vocalization in the original and degraded conditions were simulated and analyzed in the same way as recorded data.

Experimental protocol

As inserting an array of 16 electrodes in a brain structure unavoidably induces a deformation of this structure, a 30-min recovery time was allowed for the structure to return to its initial shape, then the array was slowly lowered. Time-frequency response profiles (TFRPs) were used to assess the quality of our recordings and to adjust electrode depth. For auditory cortex recordings (A1 and VRB), the recording depth was 500-1000 μm, which corresponds to layer III and the upper part of layer IV according to Wallace and Palmer (2008). For thalamic recordings, the NeuroNexus probe was lowered about 7mm below the pia before the first responses to pure tones were detected. For the collicular and cochlear nucleus recordings, the NeuroNexus probe was visually inserted into the structure and after a 15 minutes stabilization period, auditory stimuli were presented.

When a clear frequency tuning was obtained for at least 10 of the 16 electrodes, the stability of the tuning was assessed: we required that the recorded neurons displayed at least three (each lasting 6 minutes) successive similar TFRPs (i.e., with similar best frequencies) before starting the protocol. When the stability was satisfactory, the protocol was started by presenting the acoustic stimuli in the following order: We first presented the four whistles at 75 dB SPL in their original versions (in quiet), then the vocoded whistles (Voc38, Voc20 and Voc10 versions) were presented at 75 dB SPL followed by the masked vocalizations presented against the chorus then against the vocalization-shaped stationary noise at 65, 75 and 85 dB SPL. Thus, the level of the original vocalizations was kept constant (75 dB SPL), and the noise level was increased (65, 75 and 85 dB SPL). In all cases, each vocalization was repeated 20 times and all the loudness levels are in RMS value. Presentation of this entire stimulus set lasted 45 minutes. The protocol was re-started either after moving the electrode array on the cortical map or after lowering the NeuroNexus probe by at least 300 μm for subcortical structures.

Behavioral Go/No-Go discrimination task

Nine eight-weeks old C57Bl/6J mice were water-deprived (33 ml/g per day) and trained daily for 200–300 trials in a Go/No-Go task involving two of the guinea pig whistles (W1 and W3 in figure 1), one (the S+) signaling the reward (a drop of water) and the other not (the S-). The training procedures were similar to those described in previous studies (Deneux et al., 2016; Ceballo et al., 2019). Mice were head-fixed and held in a plastic tube on aluminum foil. Mice first performed 1-3

habituation sessions to learn to obtain a water reward (~5 µl) by licking on a stainless steel water spout at least 8 times after the positive stimulus S+. A trial only started when the mice were not licking the spout for at least 3 seconds. Licks were detected by changes in resistance between the aluminum foil and the water spout. After habituation, the fraction of collected rewards was ~80%. The learning protocol then started in which mice received the S− for which they had to lick less than 3 times to avoid a 5s time-out. One of the two whistles (the S+ or the S-) was presented every 10-20 s (uniform distribution) followed by a 1s test period during which the mouse had to lick at least 5-8 times to receive the reward. Positive and negative stimuli were played in a pseudorandom order with the constraint that exactly 4 positive and 4 negative sounds must be played every 8 trials. Once a mouse showed at least 80% of correct discrimination between the S+ and the S- for two successive days in the original condition, it was trained in noisy conditions, first with the stationary noise (successively at +10, 0 and -10 dB SNR), then with the chorus noise (successively at +10, 0 and -10 dB SNR). Each mouse had to perform at least one day at 80% in a given SNR to be tested on the following day at a lower SNR. Behavioral analyses were all automated; thus no animal randomization or experimenter blinding was used.

Data analysis

All the analyses were performed on MATLAB 2021 (MathWorks).

Quantification of responses to pure tones

The TFRPs were obtained by constructing post-stimulus time histograms for each frequency with 1 ms time bins. The firing rate evoked by each frequency was quantified by summing all the action potentials from the tone onset up to 100 ms after this onset. Thus, TFRPs were matrices of 100 bins in abscissa (time) multiplied by 129 bins in ordinate (frequency). All TFRPs were smoothed with a uniform 5x5 bin window for visualization (not for the data analyses). For each TFRP, the Best Frequency (BF) was defined as the frequency at which the highest firing rate was recorded. Peaks of significant response were automatically identified using the following procedure: A positive peak in the TFRP was defined as a contour of firing rate above the average level of the baseline activity (100ms of spontaneous activity taken before each tone onset) plus six times the standard deviation of the baseline activity. Recordings without significant peak of responses or with inhibitory responses (decreases in firing rate 3 standard deviations below spontaneous activity) were excluded from the data analyses.

Quantification of the envelope tracking

We first extracted the envelope as explained on a previous section (see above "Overall envelope extraction") and then filtered them (original, vocoded and noisy vocalizations) using a bank of 35 gammatone filters with center frequencies uniformly spaced along a guinea pig - adapted ERB (equivalent rectangular bandwidth) scale ranging from 20 to 30 000 Hz. Then, three ranges of amplitude modulation (AM) were investigated: the low (L, < 20 Hz), middle (M, between 20 and 100 Hz) and high (H, between 100 and 200 Hz) AM ranges. For all the AM filtering, we used Butterworth filters at -6 dB per octave. Second, the envelopes were downsampled to a resolution of 1 ms to match the sampling rate of the PSTHs. Finally, we applied a half-wave rectification followed by a normalization with the corresponding RMS value.

The neuronal responses (i.e. the PSTHs) were also filtered with the same three frequency bands as the envelopes followed by a normalization with the corresponding RMS value. The rationale for this filtering step was that we wanted to isolate and quantify the correspondence between temporal aspects of the stimuli in particular frequency ranges and PSTHs.

Next, we performed normalized cross-correlations between the filtered envelopes and PSTHs for each AM range. We selected seven gammatones, as a trade-off between accurately representing the envelopes along the audio spectrum and minimizing redundancy between envelopes. Maximal values in the correlograms were automatically detected in each structure to account for propagation delays in the auditory system. The lags were selected according to the distributions of the latencies obtained in response to pure tones at 75 dB SPL. The different lags identified were: 1-10ms for CN, 5-20ms for CNIC, 6-15ms for MGv, 9-30ms for A1 and 9-40ms for VRB. In all analyses, we decided to keep the maximal correlation coefficient out of the seven selected gammatone filters ($Rmax_{E\text{-}PSTH}$).

Evaluation of the correlation significance by shuffling the evoked activity

It is known that significant correlation between neuronal events and sensory stimuli can be obtained by chance (see for review Harris, 2020). Therefore, it was crucial to run drastic controls to reduce the probability that the correlations detected here result from spurious correlations.

To determine a significance threshold for the correlation, we shuffled only the evoked activity in the original condition on a time-scale of 1 ms, in order to preserve the global shape of the whole response (i.e., the four response peaks due to the starting of each stimulus separated by a period of silence). Specifically, for the original condition, we only shuffled the spikes obtained during the presentation of each whistle to avoid adding spikes in the silence period. The obtained shuffled PSTHs were then processed using the same procedure as for unshuffled PSTHs: filtering in the three AM ranges and half-wave rectification followed by a normalization with the corresponding

RMS value. Then, we computed the cross-correlation (R_{Random}) between each shuffled PSTH and each envelope. We performed this procedure 1000 times and set, for each correlation value PSTH-E, a significance threshold of the R value that is the mean of the R_{Random} values plus two fold the standard deviations ($\mu(R_{Random}) \pm 2\sigma$). Based upon this criterion, percentages of recordings were discarded in each structure and for each AM range: in VRB, 30%, 10%, 47% of recordings were discarded in the L, M and H range respectively; in A1, 51%, 38%, 73% of recordings were discarded in the L, M and H range respectively; in MGv, 61%, 49%, 63% of recordings were discarded in the L, M and H range respectively; in CNIC, 29%, 26%, 33% of recordings were discarded in the L, M and H range respectively; in CN, 33%, 43%, 50% of recordings were discarded in the L, M and H range respectively; in sANF, 35%, 86%, 77% of recordings were discarded in the L, M and H range respectively. Although this drastic procedure discarded a non-negligible proportion of recordings, it reduced the probability that the correlations described here were obtained by chance.

Quantification of mutual information from the responses to vocalizations

The method developed by Schnupp and colleagues (2006) was used to quantify the amount of information contained in the responses to vocalizations obtained with natural, vocoded or noisy stimuli. This method allows quantifying how well the vocalization's identity can be inferred from neuronal responses. Neuronal responses were represented using different time scales ranging from the duration of the whole response (total spike count) to a 1-ms precision (precise temporal patterns), which allows analyzing how much the spike timing contributes to the information. As this method is exhaustively described in Schnupp and colleagues (2006) and in Gaucher and colleagues (2013a), we only present below the main principles.

The method relies on a pattern-recognition algorithm that is designed to "guess which stimulus evoked a particular response pattern" (Schnupp et al., 2006) by going through the following steps: From all the responses of a subcortical or cortical site to the different stimuli, a single response (test pattern) is extracted and represented as a PSTH with a given bin size. Then, a mean response pattern is computed from the remaining responses for each stimulus class. The test pattern is then assigned to the stimulus class of the closest mean response pattern. This operation is repeated for all the responses, generating a confusion matrix where each response is assigned to a given stimulus class. From this confusion matrix, the Mutual Information (MI) is given by Shannon's formula:

$$MI = \sum_{x,y} p(x,y) \times \log_2 \left(\frac{p(x,y)}{p(x) \times p(y)} \right)$$

where x and y are the rows and columns of the confusion matrix, or in other words, the values taken by the random variables "presented stimulus class" and "assigned stimulus class".

In our case, we used responses to the four whistles and selected the first 280 ms of these responses to work on spike trains of exactly the same duration (the shortest whistle being 280 ms long). In a scenario where the responses do not carry information, the assignments of each response to a mean response pattern is equivalent to chance level (here 0.25 because we used 4 different stimuli and each stimulus was presented the same number of times) and the MI would be close to zero. In the opposite case, when responses are very different between stimulus classes and very similar within a stimulus class, the confusion matrix would be diagonal and the mutual information would tend to log2(4) = 2 bits. This algorithm was applied with different bin sizes ranging from 1 to 280 ms (see figure 2B in Souffi and colleagues (2020) for the evolution of MI with temporal precisions ranging from 1 to 40 ms). The value of 8 ms was selected for the data analysis because in each structure the MI reached its maximum at this value of temporal precision.

The MI estimates are subject to non-negligible positive sampling biases. Therefore, as in Schnupp and colleagues (2006), we estimated the expected size of this bias by calculating MI values for "shuffled" data, in which the response patterns were randomly reassigned to stimulus classes. The shuffling was repeated 100 times, resulting in 100 MI estimates of the bias (MI_{bias}). These MI_{bias} estimates are then used as estimators for the computation of the statistical significance of the MI estimate for the real (unshuffled) datasets: the real estimate is considered as significant if its value is statistically different from the distribution of MI_{bias} shuffled estimates. Significant MI estimates were computed for MI calculated from neuronal responses under one electrode and for each condition. Therefore, there was a MI_{bias} value for each MI estimate. The range of MI_{bias} values was very similar between brain structures: depending on the conditions (original, vocoded and noisy vocalizations), it ranged from 0.102 to 0.107 bits in the CN, from 0.107 to 0.110 bits in the IC, from 0.105 to 0.114 bits in the MGB, 0.107 to 0.111 bits in the A1 and from 0.106 to 0.116 bits in VRB. There was no significant difference between the mean values of MI_{bias} in the different structures (Students' t test unpaired, all $p>0.25$).

Quantification of acoustic envelope similarity

For each acoustic condition and each AM range, we quantified the acoustic similarity between each pair of stimuli as the correlation between their envelopes across the seven selected gammatones. Then, we averaged the six correlation values (related to all possible combinations with the four stimuli) to obtain an estimate of the similarity between the four stimuli for each condition (original, vocoding and noisy conditions) and each AM range (see Fig. 7A, dark lines). More precisely, we averaged Fisher z-transformed coefficients and reported the back-transformed averages on the figure 7A. In order to confirm that there is no bias in our gammatone selection, we carried out the

same analysis on the output of the 35 gammatones and obtained similar results (see Fig. 7A, light lines).

Statistical analysis

We used an analysis of variance (ANOVA) for multiple factors to reveal the main effects in the whole data set (vocoding conditions: three levels, masking noise conditions: three levels for each noise; auditory structures: six levels; AM ranges: three levels). Post-hoc pairwise tests were performed between the original condition and the vocoding or noisy conditions, or between structures to assess the significance of the multiple comparisons. They were corrected for multiple comparisons using Bonferroni corrections and were considered as significant if their p-value was below 0.05.

Results

We simulated auditory nerve fiber (sANF) responses and collected neuronal recordings from five auditory structures: the cochlear nucleus (CN, 10 animals), the central nucleus of the inferior colliculus (CNIC, 11 animals), the ventral part of the medial geniculate (MGv, 10 animals), the primary auditory cortex (A1, 11 animals) and a secondary auditory area (VRB, 5 animals).

All analyses were performed on a set of recordings (or simulated recordings) selected using stringent criteria and *n* values correspond to the number of selected recordings. Note that all the R values presented below are considered as significant (see Method section for more details).

Figures 1A-B illustrate the spectrograms and the overall envelopes of all stimuli in the original, vocoded and noisy conditions. In the following, the term stimulus refers either to the four original or vocoded whistles, or to the four whistles embedded in noise. The four overall envelopes of the stimuli were clearly different between each other in the original and vocoded conditions, however, they progressively became more similar in noisy conditions as the SNR decreased, especially in stationary noise.

Auditory neurons track the envelopes in the low AM range better than in middle and high AM ranges

We first determined which ranges of amplitude modulations are tracked by the subcortical and cortical neurons. To address this question, we filtered both the envelopes and the neuronal responses in three AM ranges: the low (< 20 Hz), middle (between 20 and 100 Hz) and high (between 100 and 200 Hz) AM ranges. Figure 1C presents the seven selected Butterworth-filtered envelopes (among the 35) of the four whistles after first having been filtered using a gammatone filterbank and brings out that the low AM range contained larger envelope fluctuations than the middle and high AM ranges. Figures 2A-B present individual examples (Fig. 2A) and populations (Fig. 2B) of PSTHs constructed from the responses to presentation of the original vocalizations in each structure. Based on these PSTHs, it appears that the evoked responses tended to be more phasic in the two cortical areas (A1 and VRB) than in the subcortical structures.

Figures 2C-E show the PSTHs from individual recordings (in black) and stimulus envelopes (E, in red) obtained in each structure (and for the sANF) in the original condition, both filtered in the same AM ranges. For each example of E-PSTH, we indicated the cross-correlation value (R) on the top left of each panel. In the following results, the correlation value selected for each recording at a given AM range was the maximum over the seven gammatone filters ($Rmax_{E\text{-}PSTH}$). Note that similar results were obtained when we used the correlation value obtained with the gammatone

filter the closest to the best frequency of each neuronal recording (data not shown). Whatever the structure, in these individual recordings, the higher R values were in the low AM range rather than in the middle and high AM ranges (Fig. 2C-E). Figure 2F presents the distribution, the mean and the interquartile range of the $Rmax_{E\text{-}PSTH}$ values for each structure in the three AM ranges (L, M and H) in the original condition. Overall, we found a statistically significant difference in average $Rmax_{E\text{-}PSTH}$ values for both the three AM ranges and the six structures (two-way ANOVA, $p < 0.05$) with a significant interaction between these two factors. For all structures, the mean $Rmax_{E\text{-}PSTH}$ values were much higher in the L range compared to the M and H ranges. In the low AM range, sANF, CN and CNIC recordings displayed significantly higher mean $Rmax_{E\text{-}PSTH}$ values than MGv and cortical recordings (one-way ANOVA, $p < 0.0001$ $F_{(5, 1165)} = 138.25$ with Students' t test unpaired, sANF vs. MGv, A1 or VRB $p<0.0001$, CN vs. MGv, A1 or VRB $p<0.0001$, CNIC vs. MGv, A1 or VRB $p<0.0001$; mean (± STD) $Rmax_{E\text{-}PSTH}$ values: $R_{sANF(n = 217)} = 0.81 \pm 0.03$, $R_{CN(n = 336)} = 0.80 \pm 0.08$, $R_{CNIC(n = 274)} = 0.78 \pm 0.11$, $R_{MGv(n = 102)} = 0.68 \pm 0.13$, $R_{A1(n = 171)} = 0.60 \pm 0.13$ and $R_{VRB(n = 66)} = 0.63 \pm 0.14$). In the middle and high AM ranges, the differences between the structures were less clear but the CNIC recordings still exhibited slightly higher mean $Rmax_{E\text{-}PSTH}$ values compared to the other structures (mean (± STD) $Rmax_{E\text{-}PSTH}$ values in the middle AM range: $R_{sANF(n = 44)} = 0.32 \pm 0.03$, $R_{CN(n = 285)} = 0.31 \pm 0.07$, $R_{CNIC(n = 285)} = 0.34 \pm 0.07$, $R_{MGv(n = 133)} = 0.31 \pm 0.07$, $R_{A1(n = 220)} = 0.27 \pm 0.05$ and $R_{VRB(n =85)} = 0.29 \pm 0.06$; mean (± STD) $Rmax_{E\text{-}PSTH}$ values in the high AM range: $R_{sANF(n = 77)} = 0.31 \pm 0.03$, $R_{CN(n = 249)} = 0.31 \pm 0.05$, $R_{CNIC(n =257)} = 0.33 \pm 0.05$, $R_{MGv(n = 97)} = 0.29 \pm 0.04$, $R_{A1(n = 196)} = 0.27 \pm 0.05$ and $R_{VRB(n =50)} = 0.30 \pm 0.05$). This poor ability to follow fast AM changes was expected for auditory cortex neurons but not expected for subcortical neurons and for sANF (which can synchronize at higher AM rates when tested with periodic artificial stimuli, review in Joris et al., 2004). This suggests that only a partial encoding of high AM rates contained in complex natural sounds is performed by subcortical neurons.

To summarize, in the original condition, the neurons' PSTHs were more strongly correlated with the stimulus envelope in the low AM range than in the middle and high AM ranges, both at the subcortical and cortical levels.

In the original condition, the better cortical and subcortical neurons track the slow envelope (<20 Hz), the higher the value of mutual information

Does envelope tracking allow auditory neurons to discriminate the four vocalizations in the original condition? To address this question, we examined whether there is a relationship between the neuronal discrimination performance and the neurons' abilities to follow the stimulus envelope (Fig. 3). The distribution, the mean and the interquartile range of the neuronal discrimination

(quantified by the mutual information, MI) are presented for each structure in Figure 3A. As previously reported (Souffi et al., 2020), subcortical neurons (CN, CNIC and MGv neurons) were better in discriminating the original whistles compared to cortical neurons (A1 and VRB neurons) and here we extended this result to sANF (one-way ANOVA $p < 0.0001$ $F_{(5, 1538)} = 266.46$ with Students' t test unpaired, sANF vs. A1 or VRB $p<0.0001$, CN vs. A1 or VRB $p < 0.0001$, CNIC vs. A1 or VRB $p < 0.0001$, MGv vs. A1 or VRB $p < 0.0001$; mean (± STD) MI values: $MI_{sANF(n = 77)}$= 1.84 ± 0.21 bits, $MI_{CN(n = 249)}$= 0.92 ± 0.47 bits, $MI_{CNIC(n =257)}$= 1.00 ± 0.5 bits, $MI_{MGv(n = 97)}$= 1.19 ± 0.55 bits, $MI_{A1(n = 196)}$= 0.68 ± 0.37 bits and $R_{VRB(n =50)}$= 0.55 ± 0.29 bits, Fig. 3A). The scattergrams presented in Figure 3B display the $Rmax_{E\text{-}PSTH}$ values as a function of the MI values in each structure and AM range.

Figure 3C summarizes the correlation values between $Rmax_{E\text{-}PSTH}$ and MI parameters, in each structure and in the three AM ranges. All significant correlation values between these two variables are reported in red. In all but one case (in CNIC in the middle AM range), significant positive correlations between $Rmax_{E\text{-}PSTH}$ and MI values were obtained in all AM ranges in subcortical structures ($p^L_{CN} < 0.0001$, $p^M_{CN}< 0.0001$, $p^H_{CN}= 0.01$, $p^L_{CNIC}< 0.0001$, $p^M_{CNIC}= 0.24$, $p^H_{CNIC}= 0.005$, $p^L_{MGv}= 0.006$, $p^M_{MGv}< 0.0001$, $p^H_{MGv}= 0.01$). For the sANF, the range of MI values was too limited to compute reliable correlations (most MI values were close to the maximum of 2 bits). At the subcortical level, the highest correlation values between $Rmax_{E\text{-}PSTH}$ and MI values as a whole, were found in MGv. At the cortical level, significant correlations between $Rmax_{E\text{-}PSTH}$ and MI values were detected in the low and middle AM ranges in A1 ($p^L_{A1} = 0.01$, $p^M_{A1}= 0.05$, $p^H_{A1}= 0.32$) and there was no significant correlation in VRB (may be as a consequence of fewer recordings in this area, $p^L_{VRB}= 0.31$, $p^M_{VRB}= 0.51$, $p^H_{VRB}= 0.99$). Interestingly, at each level except in VRB, there was a positive and significant correlation value in the low AM range suggesting that the neuronal ability for tracking the slow envelopes (<20 Hz) better explains the neuronal discrimination in the entire auditory system than the tracking of higher AM rates.

To summarize, it appeared that in the original condition, the better the tracking of the temporal envelope, the better the between-stimuli neuronal discrimination. In addition, for cortical neurons, the correlation between the $Rmax_{E\text{-}PSTH}$ and MI values was stronger in the lower AM range, whereas for subcortical neurons, there were also still significant correlations in the higher AM ranges.

The acoustic degradations decreased the values of mutual information but did not affect the envelope tracking performed by the auditory neurons

In almost all situations of acoustic degradations, the neurons' ability to discriminate between the four vocalizations was decreased. Figures 4A-F present the distributions of the MI values for the original condition and the three levels of degradation conditions: the three tone-vocoders (38, 20 and 10 frequency bands) or the three SNRs (+10, 0 and -10 dB SNR) in the two types of noise (stationary and chorus noises). In general, there were modest effects on the MI values in the vocoding and chorus noise conditions compared to the stationary noise conditions for all structures except sANF. The decrease was significant only for the 10-band vocoded vocalizations in MGv and A1 (Fig. 4D, one-way ANOVA, $p = 0.05$ $F_{(3, 811)} = 2.58$ with Students' t test paired, MGv_{Ori} vs. MGv_{Voc10} $p < 0.0001$, mean (± STD) MI values: $MI_{Ori} = 1.19 \pm 0.55$ bits, $MI_{Voc38} = 1.13 \pm 0.57$ bits, $MI_{Voc20} = 1.15 \pm 0.55$ bits, $MI_{Voc10} = 1.03 \pm 0.53$ bits; Fig. 4E, one-way ANOVA, $p = 0.001$ $F_{(3, 722)} = 3.73$ with Students' t test paired, $A1_{Ori}$ vs. $A1_{Voc10}$ $p < 0.0001$, mean (± STD) MI values: $MI_{Ori} = 0.68 \pm 0.37$ bits, $MI_{Voc38} = 0.62 \pm 0.33$ bits, $MI_{Voc20} = 0.61 \pm 0.33$ bits, $MI_{Voc10} = 0.56 \pm 0.30$ bits), and no significant difference was detected in VRB (Fig.4F, one-way ANOVA, $p = 0.75$ $F_{(3, 186)} = 0.41$, mean (± STD) MI values: $MI_{Ori} = 0.55 \pm 0.29$ bits, $MI_{Voc38} = 0.55 \pm 0.28$ bits, $MI_{Voc20} = 0.55 \pm 0.29$ bits, $MI_{Voc10} = 0.61 \pm 0.31$ bits). However, the decrease was already significant with 38-band vocoded vocalizations in sANF or with 20-band vocoded vocalizations in CN and CNIC (Fig.4A, one-way ANOVA, $p < 0.0001$ $F_{(3, 1302)} = 111.3$ with Students' t test paired, $sANF_{Ori}$ vs. $sANF_{Voc38}$ $p < 0.0001$, mean (± STD) MI values: $MI_{Ori} = 1.84 \pm 0.21$ bits, $MI_{Voc38} = 1.61 \pm 0.32$ bits, $MI_{Voc20} = 1.39 \pm 0.52$ bits, $MI_{Voc10} = 1.29 \pm 0.52$ bits; Fig.4B, one-way ANOVA, $p < 0.0001$ $F_{(3, 1424)} = 12.42$ with Students' t test paired, CN_{Ori} vs. CN_{Voc20} $p < 0.0001$, mean (± STD) MI values: $MI_{Ori} = 0.92 \pm 0.47$ bits, $MI_{Voc38} = 0.96 \pm 0.46$ bits, $MI_{Voc20} = 0.86 \pm 0.45$ bits, $MI_{Voc10} = 0.75 \pm 0.43$ bits; Fig.4C, one-way ANOVA, $p < 0.0001$ $F_{(3, 1231)} = 13.17$ with Students' t test paired, $CNIC_{Ori}$ vs. $CNIC_{Voc20}$ $p < 0.0001$, mean (± STD) MI values: $MI_{Ori} = 1.00 \pm 0.49$ bits, $MI_{Voc38} = 0.99 \pm 0.46$ bits, $MI_{Voc20} = 0.90 \pm 0.46$ bits, $MI_{Voc10} = 0.79 \pm 0.39$ bits). Note that there was also a significant increase in MI values with the 38-band vocoded vocalizations in CN (Fig.4B, one-way ANOVA, $p < 0.0001$ $F_{(3, 1424)} = 12.42$ with Students' t test paired, CN_{Ori} vs. CN_{Voc38} $p= 0.0073$).

In chorus noise, in CN and CNIC, there was no significant decrease in mean MI values (Fig. 4B, one-way ANOVA, $p = 0.05$ $F_{(3, 1176)} = 2.65$, mean (± STD) MI values: $MI_{Ori} = 0.92 \pm 0.47$ bits, $MI_{+10dB} = 0.85 \pm 0.48$ bits, $MI_{0dB} = 0.83 \pm 0.50$ bits, $MI_{-10dB} = 0.83 \pm 0.49$ bits; Fig. 4C, one-way ANOVA, $p = 0.36$ $F_{(3, 1188)} = 1.06$, $MI_{Ori} = 1.00 \pm 0.49$ bits, $MI_{+10dB} = 1.05 \pm 0.50$ bits, $MI_{0dB} = 1.06 \pm 0.52$ bits, $MI_{-10dB} = 1.06 \pm 0.52$ bits), whereas in sANF and MGv, the mean MI values significantly decreased at +10 dB or 0 dB SNR respectively (Fig. 4A, one-way ANOVA, $p < 0.0001$ $F_{(3, 1331)} = 232.86$ with Students' t test paired, $sANF_{Ori}$ vs. $sANF_{+10dB}$ $p < 0.0001$, mean (± STD) MI values: $MI_{Ori} = 1.84 \pm 0.21$ bits, $MI_{+10dB} = 1.48 \pm 0.37$ bits, $MI_{0dB} = 1.20 \pm 0.45$ bits, $MI_{-10dB} = 1.09 \pm 0.50$ bits; Fig. 4D, one-way ANOVA, $p < 0.0001$ $F_{(3, 753)} = 7.3$ with Students' t test

paired, MGv_{Ori} vs. MGv_{0dB} $p < 0.0001$, mean (± STD) MI values: $MI_{Ori} = 1.19 \pm 0.55$ bits, $MI_{+10dB} = 1.08 \pm 0.52$ bits, $MI_{0dB} = 0.99 \pm 0.50$ bits, $MI_{-10dB} = 0.98 \pm 0.48$ bits). At the cortical level, there was a significant decrease in A1 at 0 dB SNR and no significant change of mean MI values in VRB (Fig. 4E, one-way ANOVA, $p = 0.0039$ $F_{(3, 697)} = 4.5$ with Students' t test paired, $A1_{Ori}$ vs. $A1_{0dB}$ $p < 0.0001$, mean (± STD) MI values: $MI_{Ori} = 0.68 \pm 0.37$ bits, $MI_{+10dB} = 0.64 \pm 0.36$ bits, $MI_{0dB} = 0.55 \pm 0.30$ bits, $MI_{-10dB} = 0.60 \pm 0.31$ bits; Fig.4F, one-way ANOVA, $p = 0.31$ $F_{(3, 179)} = 1.19$, mean (± STD) MI values: $MI_{Ori} = 0.55 \pm 0.29$ bits, $MI_{+10dB} = 0.63 \pm 0.32$ bits, $MI_{0dB} = 0.54 \pm 0.27$ bits, $MI_{-10dB} = 0.53 \pm 0.24$ bits).

Stationary noise strongly reduced the MI values compared to the vocoding and the chorus noise addition. The mean MI value in sANF, CN and MGv was significantly reduced already at +10 dB SNR (Fig. 4A, one-way ANOVA, $p < 0.0001$ $F_{(3, 1153)} = 767.64$ with Students' t test paired, $sANF_{Ori}$ vs. $sANF_{+10dB}$ $p < 0.0001$, mean (± STD) MI values: $MI_{Ori} = 1.84 \pm 0.21$ bits, $MI_{+10dB} = 1.09 \pm 0.39$ bits, $MI_{0dB} = 0.68 \pm 0.37$ bits, $MI_{-10dB} = 0.66 \pm 0.39$ bits; Fig. 4B, one-way ANOVA, $p < 0.0001$ $F_{(3, 812)} = 61.22$ with Students' t test paired, CN_{Ori} vs. CN_{+10dB} $p < 0.0001$, mean (± STD) MI values: $MI_{Ori} = 0.92 \pm 0.47$ bits, $MI_{+10dB} = 0.68 \pm 0.38$ bits, $MI_{0dB} = 0.53 \pm 0.26$ bits, $MI_{-10dB} = 0.41 \pm 0.17$ bits; Fig. 4D, one-way ANOVA, $p < 0.0001$ $F_{(3, 630)} = 62.03$ with Students' t test paired, MGv_{Ori} vs. MGv_{+10dB} $p < 0.0001$, mean (± STD) MI values: $MI_{Ori} = 1.19 \pm 0.55$ bits, $MI_{+10dB} = 1.00 \pm 0.50$ bits, $MI_{0dB} = 0.74 \pm 0.35$ bits, $MI_{-10dB} = 0.46 \pm 0.19$ bits), whereas the mean MI value in CNIC was significantly reduced at 0 dB SNR (Fig. 4C, one-way ANOVA, $p < 0.0001$ $F_{(3, 1078)} = 32.08$ with Students' t test paired, $CNIC_{Ori}$ vs. $CNIC_{0dB}$ $p < 0.0001$, mean (± STD) MI values: $MI_{Ori} = 1.00 \pm 0.49$ bits, $MI_{+10dB} = 1.00 \pm 0.49$ bits, $MI_{0dB} = 0.87 \pm 0.44$ bits, $MI_{-10dB} = 0.63 \pm 0.28$ bits). At the cortical level, noise significantly reduced the mean MI value in A1 only at -10 dB SNR (Fig. 4E, one-way ANOVA, $p < 0.0001$ $F_{(3, 669)} = 13.99$ with Students' t test paired, $A1_{Ori}$ vs. $A1_{-10dB}$ $p < 0.0001$, mean (± STD) MI values: $MI_{Ori} = 0.68 \pm 0.37$ bits, $MI_{+10dB} = 0.62 \pm 0.34$ bits, $MI_{0dB} = 0.59 \pm 0.31$ bits, $MI_{-10dB} = 0.42 \pm 0.18$ bits), whereas the mean MI values in VRB remained unchanged in all conditions (Fig. 4F, one-way ANOVA, $p = 0.26$ $F_{(3, 164)} = 1.34$, mean (± STD) MI values: $MI_{Ori} = 0.55 \pm 0.29$ bits, $MI_{+10dB} = 0.55 \pm 0.28$ bits, $MI_{0dB} = 0.51 \pm 0.22$ bits, $MI_{-10dB} = 0.42 \pm 0.17$ bits).

What can be the scenarios explaining the decrease in neuronal discrimination and involving the envelope tracking in situations of acoustic degradations? At least two scenarios can be envisioned: First, in a condition-independent envelope tracking scenario, a neuron keeps the same intrinsic capacity to track the stimulus envelopes whatever the acoustic conditions, i.e., both in quiet and in conditions of acoustic degradations. In that case, as long as the stimulus envelopes present some differences, the neuron will detect these differences and will discriminate the stimuli. Second, in a condition-dependent scenario, the acoustic degradations reduce the neurons' ability to track the stimulus envelope. In that case, despite differences between the stimulus envelopes, the intense

activity occurring when the neurons are strongly driven by the noise prevents the recorded neuron from tracking the stimulus envelopes. To determine which of these two scenarios actually operates, we investigated whether the $Rmax_{E\text{-}PSTH}$ values were changed in the conditions of acoustic degradations such as the vocoding or the noise addition (Figures 5-6). Figure 5 shows, for individual recordings, the superpositions of the PSTH and the envelope (E) in the low AM range for the original condition and all the degraded conditions (vocoding, stationary and chorus noise) in each auditory structure. The $Rmax_{E\text{-}PSTH}$ values are indicated on the top left of each panel. In these individual recordings, the $Rmax_{E\text{-}PSTH}$ values presented very little changes in all degraded conditions compared to the original condition.

We next quantified for each recording, the $Rmax_{E\text{-}PSTH}$ variations compared with the original condition ($\Delta Rmax_{E\text{-}PSTH}$). This was quantified in each structure, for all the degraded conditions and each AM range (Fig. 6). Compared with the $Rmax_{E\text{-}PSTH}$ values obtained in the original condition, there was little or no change in the degraded conditions for all structures. More precisely, in sANF and CN, we observed a maximal increase in mean (± STD) $Rmax_{E\text{-}PSTH}$ values of 0.16 (±0.03) (and 0.11 (±0.13) for CN) and, a maximal decrease of 0.10 (±0.04) (and 0.05 (±0.06) for CN) depending on the degraded conditions and the AM range (Fig. 6). In CNIC and MGv, the mean (± STD) $Rmax_{E\text{-}PSTH}$ changes in degraded conditions were very small (Fig. 6, between -0.06 (±0.03) and 0.006 (±0.06) for CNIC and between -0.08 (±0.08) and -0.0002 (±0.15) for MGv). In A1, the changes in mean (± STD) $Rmax_{E\text{-}PSTH}$ values varied between -0.09 (±0.11) and 0.07 (±0.15) and in VRB it varied between -0.13 (±0.13) and 0.07 (± 0.15).

These results clearly provide evidence that the abilities of neurons for tracking the temporal envelope cues were preserved at each level of the auditory system and in all the situations of acoustic degradations.

The increase in between-envelope similarity explains the decrease in neuronal discrimination

If the neurons are still able to track the stimulus envelopes in all conditions of acoustic degradations, what could explain the pronounced MI decrease in these situations? The most parsimonious explanation is that the noise addition increases the similarity between stimulus envelopes, which in turn reduces the neuronal discriminative efficiency based on the envelope tracking. We thus quantified the acoustic similarity between the stimulus envelopes in the original condition and in all situations of acoustic degradations. The changes of the between-envelope similarity in each AM range are presented in figure 7A. In the M and H ranges, the between-stimulus envelope similarity was low and remained low in all degraded conditions. In contrast, large changes occurred in the low AM range: in these frequency ranges, the envelope similarity

increased progressively with the acoustic degradations. In the following results, we will focus on this AM range.

In the vocoding conditions, the similarity between the four whistle envelopes was relatively constant, except for the 10-band vocoded condition where this similarity was slightly higher. In the stationary noise, the four stimulus envelopes became similar and reached a correlation value above 0.8 at the -10 dB SNR condition (which is very close to the maximal value of the acoustic similarity). In the chorus noise conditions, the four stimulus envelopes remained different (because spectro-temporal differences were present in the frozen chorus noise) with the highest similarity in the -10 dB SNR condition.

Figure 7B points out that in the condition where the between-stimulus envelope similarity was higher (at -10 dB SNR in stationary noise), the envelope tracking remained similar (the $\Delta Rmax_{E\text{-}PSTH}$ values remained stable) whereas the neuronal discrimination decreased compared to the original condition (most of the ΔMI values were largely negative). This clearly demonstrates the dissociation between changes in Rmax value and those in MI value. Figure 7C highlights the close relationship between the acoustic similarity of the four stimulus envelopes and the abilities of auditory neurons to discriminate between them. Both in subcortical and cortical structures, as the acoustic distance between the four stimulus envelopes in the low AM range progressively decreased, the neuronal discrimination decreased (Fig. 7C).

Together, these results indicate that it is not a loss in neuronal envelope tracking which leads to a reduction of the neuronal discriminative abilities in the degraded conditions. Rather, it is the increase in envelope similarity in situation of acoustic degradations that is one of the important factors responsible for the decrease in discrimination abilities. Thus, the between-stimulus envelope similarity in the lower AM range (<20 Hz) can predict the evolution of the discrimination in the entire auditory system.

The increase in between-envelope similarity also correlates with the behavioral performance in noise

To examine whether the discrimination performance of auditory neurons might provide a neuronal basis for behavioral performance, we tested whether behaving animals can discriminate between whistles when engaged in an operant conditioning task involving the same stimuli. We opted to train mice in a behavioral task rather than guinea pigs for two main reasons: (1) guinea pigs are poor and slow learners in instrumental tasks (2) this avoided that the stimuli used for the behavioral task have innate particular meanings because whistles are alert signals for guinea pigs.

The behavioral task was a Go/No-Go task involving the discrimination between two of the four whistles used in our electrophysiological studies (W1 and W3 see figure 1): Licks to the S+ were rewarded by a 5µL drop of water and licks to the S- were punished by a 5-second time-out period. Mice were first trained for 5-10 initial sessions to perform the discrimination in the original condition until they reached 80% of correct responses for two successive days (N = 9). Then, the mice were sequentially trained in the stationary noise at the +10, 0 and -10 dB SNR for at least four sessions. The performance at the last four sessions at each SNR are displayed on figure 7D. For all mice, the average performance decreased at the 0 and -10 dB SNR, even if two mice were still at 80% of correct performance, the others were slightly above the chance level. In the chorus noise, the performance of most of the mice were relatively stable, which can be explained by the fact that acoustically the chorus noise surrounding the two target vocalizations differed between the two whistles, so that there were more acoustic cues to discriminate between the target stimuli in these conditions (note that this could also come from the fact that the mice were already extensively trained to perform the discrimination task in stationary noise when they started the chorus noise). Despite this pitfall, the main result of this behavioral study was that mice can discriminate the target vocalizations above chance level even at -10 dB SNR in stationary noise. Furthermore, the decrease in behavioral performance was strongly related to the reduction of the differences between the two temporal envelopes in the low AM range (inset in Fig. 7D). These results provide evidence that the behavioral performance of mice is correlated with the changes in the slow temporal envelope cues.

Discussion

Our first major result is that the neuronal discrimination performance in the original condition was correlated with the capacity for tracking the envelopes in the low AM range both for subcortical and cortical neurons, except in the secondary auditory cortex (VRB) (Fig. 3C). Our second major result is that, under acoustic degraded conditions and in each structure, the ability for envelope tracking only slightly changed compared to the original condition (Fig. 5, 6, 7B). Finally, our findings revealed that the increased similarity between the stimulus envelopes in the low AM range (<20 Hz, Fig. 7C-D) is one of the important factors responsible for the decrease in neuronal and behavioral discrimination.

Slow envelope tracking: a general property of auditory neurons

At the level of the auditory nerve, previous studies reported conflicting results concerning the noise resistance: Frisina and colleagues (1996) found that all AN units partially preserve their AM coding even in the presence of loud (0 or +6 dB SNR) background noise. However, many others electrophysiological studies, and the present simulated data, showed a low resistance to noise in the auditory nerve (Rhode et al., 1978; Geisler and Sinex, 1980; Palmer and Evans, 1982; Costalupes et al., 1984; Costalupes, 1985; Young and Barta, 1986). This can be explained by several factors including (i) the type of target stimuli (artificial vs. natural stimuli), (ii) the noise type (stationary vs. non-stationary noise), (iii) the type of the auditory nerve fibers (low, middle and high SR fibers), and also the noise levels which have been tested. For example, electrophysiological studies have shown that low and medium SR fibers with best frequencies around the frequency of a pure tone exhibited tone-evoked rate changes in presence of a stationary noise at positive SNRs (Rhode et al., 1978; Geisler and Sinex, 1980; Palmer and Evans, 1982; Costalupes et al., 1984; Costalupes, 1985; Young and Barta, 1986). High SR fibers, in contrast, exhibited much weaker tone-evoked rate changes at positive SNRs limited by the high rate response to noise. Thus, as noise level increases, the discharge rate approaches a fiber's saturation rate and ultimately eliminates the fiber's ability to respond to tested tones. Low (and middle) SR fibers that have higher thresholds and wider dynamic range, are significantly more resistant to saturation by high noise levels than high SR fibers. Therefore, a different ratio between low, middle and high SR fibers could have changed our results in a way that more sANF responses showed a higher resistance to noise. Here, as we wanted to be as close as possible to the multi-unit activity recorded in the auditory structures (we assumed that we recorded about 5 neurons under each electrode), we decided to choose five fibers with a classical ratio of 1 low SR fiber, 1 medium SR fiber and 3 high SR fibers. However, we should

keep in mind that all these previous studies have used tones (or amplitude modulated tones) in noise at positive SNRs, but natural sounds can potentially trigger more complex encoding as early as the auditory nerve. Recently, using a similar model of auditory nerve as in the present study, Rabinowitz and colleagues (2013) showed a poor adaptation to the noise statistics by simulated fibers when natural environment sounds were used as target stimuli whereas auditory cortex and IC neurons showed a better adaptation to noise. In our study, we also found a high sensitivity to the noise for sANF as early as +10 dB SNR in both noises (see examples on Figure 5) and also in the vocoding conditions potentially due to a higher sensitivity to the spectrotemporal alterations compared to the other structures (see figure 4A).

A few electrophysiological studies have shown that subcortical neurons can display responses very close to the envelopes of natural stimuli (inferior colliculus: Suta et al., 2003; Rode et al., 2013; MGB: Tanaka and Taniguchi, 1991; Philibert et al., 2005; Suta et al., 2007). Rode and colleagues (2013) found that between 15 and 60% of collicular neurons displayed high correlations for at least one of the three vocalization envelopes, and a subset of collicular neurons even followed the envelopes of the three guinea pig vocalizations with high correlations (>0.85). A similar range of correlations (between 0.6-0.9) in CNIC was obtained in the present study and, as in their study, we also did not find a relation between the gammatone filter eliciting the highest $R_{E\text{-}PSTH}$ value and the best frequency of the neurons.

Unlike to other previous cortical studies (Wang et al., 1995; Bar-Yosef et al., 2002; Nagarajan et al., 2002; Grimsley et al., 2012; Abrams et al., 2017), we filtered envelopes and neuronal responses in the same frequency bands - from low (<20 Hz) to high (100 and 200 Hz) ranges - to obtain a direct quantification of the envelope tracking abilities in particular frequency ranges. Furthermore, we compared the degree of envelope tracking performed by subcortical and cortical neurons in challenging situations where the envelope is either relatively well preserved or strongly degraded. Nagarajan and colleagues (2002) found that the synchronization between A1 responses and the temporal envelope of vocalizations was highly significant and, interestingly, this property was underestimated based on responses to amplitude-modulated tones. In addition, they pointed out that A1 responses were quite resistant to spectral degradations (generated by a noise-vocoder) and to noise addition up to 0 dB SNR. More importantly, the responses were similar when the vocalization envelope was preserved between 2 and 30 Hz, whereas the responses were strongly reduced when the envelope was low-pass filtered at 4 or 10 Hz. We confirmed these cortical results on several aspects: first, the highest correlation coefficients were detected in the lower AM range (<20 Hz) for each acoustic condition, second, we showed that the envelope tracking ability was little affected by the presence of noise addition or by the vocoding. We extended these results to a non-primary cortical area (VRB), to each subcortical level, and even to sANF. Note that the envelope tracking

ability is not specific to the processing of conspecific vocalizations: similar results were found with speech in noise in the auditory cortex of guinea pigs (Abrams et al., 2017).

Together, these results highlight that subcortical and cortical auditory neurons maintain their capacity to track the slow envelope of natural sounds both when they are composed of noise-free vocalizations or a mixture of noise and vocalizations, suggesting that this property is immutable and unchanged by the acoustic degradations.

In the low AM range (<20 Hz), we noticed a decrease in mean correlation ($Rmax_{E\text{-}PSTH}$) values from midbrain to thalamus to cortex (Fig. 2F) reflecting that the further away from the periphery, the less precise is the phase-locking ability on the AM cues. For higher AM rates, we expected higher correlations between the neuronal responses and the envelopes for subcortical structures (Creutzfeldt et al., 1980; Frisina et al., 1990; Rhode and Greenberg, 1994; Neuert et al., 2001; for review, Joris et al., 2004). Surprisingly, such a hierarchy was not detected in our results, the mean correlations in higher AM rates (>20 Hz) being similarly low for each structure including the sANF. These lower correlation coefficients obtained for the middle- and high-AM frequency bands for all structures, might result because the envelopes have much lower amplitudes in these bands than in the low-AM frequency band (see Figure 1C). Another hypothesis is that shorter segments of neuronal responses could be highly correlated to the higher AM ranges of the envelopes. If so, reducing the time window on which the correlation is computed should increase the correlations in the higher AM ranges. We computed the cross-correlation for each whistle (around 300 ms) and still found low correlations in higher AM ranges (data not shown). This suggests that if higher correlations exist in higher AM ranges, smaller temporal windows (less than several hundreds of milliseconds) are required to reveal them. The fact that Abrams and colleagues (2017) found some residues of the fundamental frequency (between 100-120 Hz, relative to the pitch) in segments of A1 responses no longer than 100 ms argues in favor of this possibility.

The main hypothesis of our study was that the tracking abilities of auditory neurons is one of the mechanisms explaining the neuronal discrimination. Another possibility is that for higher AM cues, some auditory neurons respond by increasing their firing rate. This hypothesis relies on the existence of a rate-place code for periodicity: whereas the temporal tracking abilities decrease along the auditory pathway, higher periodicities can be encoded by a rate-place code as this has been demonstrated using amplitude modulated sounds in different species (Langner & Schreiner, 1988; Schreiner & Langner, 1988; Langner, 1992; Lu et al., 2001a, b; Liang et al., 2002; Lu and Wang, 2004). According to this possibility, neurons increasing their firing rate for coding higher AM cues should be located at particular locations in IC and auditory cortex (Langner et al., 2009; Schnupp et al., 2015). However, in order to explain the neuronal discrimination, it seems necessary that each of the four whistles activated different locations in the periodicity maps of the different auditory

structures. As shown in figure 1C, each of the four whistles contained about the same energy in low, middle and high AM modulations, and as a consequence similar locations should be activated in these periodicity maps leading to a low discrimination level. Thus, although we cannot discard this hypothesis, the possibility that the neural discrimination relies on a rate-place code for particular AM cues seems unlikely. At the cortical level (both in A1 and in VRB), it is also possible that despite the fact individual neurons cannot keep tracking the detailed envelope fluctuations (because of their low-pass properties regarding AM cues and their prominent onset responses), they may, as a large population, track the envelope changes if each neuron is sensitive to a particular rate of change of the stimulus envelope (a particular rate of transients). Note that according to this hypothesis, which has been formulated almost twenty years ago (Heil, 2003), this tracking mechanism would also lose accuracy with increasing levels of background noise.

The decrease in neuronal discrimination can be explained by the increase of between-envelopes similarities in the low AM range

In the original condition, the better neurons track the slow envelope (<20 Hz), the higher the neuronal discrimination performance for all structures (Fig. 3B-C). In situations of acoustic degradation, the envelopes of the original stimuli were altered leading to situations where the envelopes were mostly dominated by the noise envelopes. However, the three situations of acoustic degradations used here notably differed. In the tone-vocoder situation, the spectral content is strongly degraded but the slow temporal envelope is relatively well preserved (Shannon et al., 1995; Kates, 2011; Souffi et al., 2020). In the chorus noise, there was only a small increase in acoustic similarity in the low AM range (Fig. 7A) because the chorus noise itself contains strong temporal variations which differ from one whistle to another. As a consequence of this pitfall, when the target vocalizations were inserted in the chorus noise, specific regions in the spectro-temporal domain were dominated by the target vocalizations, while in other regions, it was dominated by the chorus noise. Consequently, the target vocalizations embedded in the chorus noise generated stimuli that can be discriminated at all SNRs either based on the vocalization envelopes or based on the chorus noise envelope itself. In all structures, the neuronal discrimination showed little decrease in the chorus noise (see Fig. 4) and so was the behavioral performance (Fig. 7D). Only in the stationary noise, the four slow envelopes became closer as the level of degradation increased (< 20 Hz, see Fig. 7A). This was detrimental for discriminating the vocalizations in noisy conditions in which envelope tracking become inefficient and worst, can strongly reduce the neuronal discrimination along the auditory system. Therefore, reducing or increasing the envelope differences in the low AM range would constrain or facilitate the neuronal discrimination in

subcortical and cortical levels. Furthermore, the behavioral performance of mice revealed that they can discriminate the target vocalizations in quiet (with > 90% correct performance) and can even discriminate the vocalizations up to 0 dB SNR in stationary noise (with 70-80% correct performance), suggesting that the between-stimulus envelope differences could explain the behavioral performance during a discrimination task. Previous studies have reported good behavioral discrimination performance in conditions of acoustic degradations such as vocoded consonants or vowels (Ranasinghe et al., 2012a, b), consonants in various levels of background noise (Shetake et al., 2011), bird songs embedded in stationary and chorus noise (Narayan et al., 2007) or in broadband dynamic moving ripples (Homma et al., 2020). In all these studies, the discrimination performance of auditory cortex neurons, based upon spike-timing, has been found to match relatively well the behavioral performance (Narayan et al., 2007; Ranasinghe et al., 2012a; Homma et al., 2020) and sometimes even with performance of human subjects (Walker et al., 2008). Altogether, our results indicate that it is not a loss in neuronal envelope tracking which leads to a reduction of the neuronal discriminative abilities in the degraded conditions, rather, it is the direct consequence of the acoustic distance changes between stimulus envelopes.

Comparison with human studies: case of newborn infants

Speech envelope corresponds to the slow amplitude fluctuations of the signal over time, with peaks occurring roughly at the syllabic rate. The two pioneer results supporting the view that the envelope plays a key role in speech comprehension are (1) that comprehension is impaired when the speech envelope is filtered out (Drullman et al., 1994a, b), and (2) that adult listeners readily understand degraded speech in which only the envelope is preserved, at least when speech is presented in silence (Shannon et al., 1995). Additionally, studies have shown that when adults listen to speech, their neuronal activity synchronized with specific features of the envelope, a phenomenon known as speech envelope tracking (Ahissar et al., 2001; Luo and Poeppel, 2007; Abrams et al., 2008; Nourski et al., 2009). Several recent electrophysiological results have provided new insights into this putative speech envelope tracking mechanism. First, oscillations whose frequency corresponds to the modulation frequency of the speech envelope (4-5 Hz) have been found to be independent of comprehension: brain responses in the theta band track the speech envelope even when speech is time-compressed at a rate that renders it incomprehensible for adult listeners (Zoefel and VanRullen, 2016; Kösem et al., 2016, 2017; Pefkou et al., 2017). Results from newborns and young infants have also brought new insights. For example, combining hemodynamic (near-infrared spectroscopy) and EEG recordings, Cabrera and Gervain (2020) showed that infants (9-10 months old) detect consonant changes on the basis of envelope cues (without the temporal fine structure)

and they can even do so on the basis of the slow temporal variation alone (AM <8 Hz). More recently, Ortiz-Barajas and colleagues (2021) found that the cortical networks of newborns (exclusively exposed to French before birth) have the capacity to track the amplitude and the phase of the speech envelope in their native languages as well as in unfamiliar languages (Spanish and English). Altogether, these results suggest that amplitude - and phase-tracking take place in the absence of attention and comprehension.

Thus, envelope tracking can be viewed as a universal mechanism used in all species to discriminate between communication sounds in a large diversity of acoustic situations ranging from quiet to adverse, challenging, conditions.

References

Abrams DA, Nicol T, Zecker S, Kraus N (2008) Right-hemisphere auditory cortex is dominant for coding syllable patterns in speech. J Neurosci. Apr 9;28(15):3958-65. doi: 10.1523/JNEUROSCI.0187-08.2008.

Abrams DA, Nicol T, White-Schwoch T, Zecker S, Kraus N (2017) Population responses in primary auditory cortex simultaneously represent the temporal envelope and periodicity features in natural speech. Hear Res. May;348:31-43. doi: 10.1016/j.heares.2017.02.010.

Ahissar E, Nagarajan S, Ahissar M, Protopapas A, Mahncke H, & Merzenich MM (2001) Speech comprehension is correlated with temporal response patterns recorded from auditory cortex. Proceedings of the National Academy of Sciences of the United States of America, 98(23), 13367–13372. doi:10.1073/pnas.201400998

Anderson LA, Wallace MN & Palmer AR (2007) Identification of subdivisions in the medial geniculate body of the guinea pig. Hearing Research 228, 156–167.

Aushana Y, Souffi S, Edeline JM, Lorenzi C, Huetz C (2018) Robust Neuronal Discrimination in Primary Auditory Cortex Despite Degradations of Spectro-temporal Acoustic Details: Comparison Between Guinea Pigs with Normal Hearing and Mild Age-Related Hearing Loss. J. Assoc. Res. Otolaryngol. 19, 163–180.

Bar-Yosef O, Rotman Y, Nelken I (2002) Responses of neurons in cat primary auditory cortex to bird chirps: effects of temporal and spectral context. J Neurosci. Oct 1;22(19):8619-32. doi: 10.1523/JNEUROSCI.22-19-08619.2002.

Bruce IC, Erfani Y, and Zilany MSA (2018) "A phenomenological model of the synapse between the inner hair cell and auditory nerve: Implications of limited neurotransmitter release sites," Hearing Research 360:40–54.

Cabrera L, Gervain J (2020) Speech perception at birth: The brain encodes fast and slow temporal information. Sci Adv. Jul 22;6(30):eaba7830. doi: 10.1126/sciadv.aba7830.

Ceballo S, Piwkowska Z, Bourg J, Daret A, Bathellier B (2019) Targeted Cortical Manipulation of Auditory Perception. Neuron. Dec 18;104(6):1168-1179.e5. doi: 10.1016/j.neuron.2019.09.043.

Costalupes JA (1985) Representation of tones in noise in the responses of auditory nerve fibers in cats. I. Comparison with detection thresholds. J Neurosci. Dec;5(12):3261-9. doi: 10.1523/JNEUROSCI.05-12-03261.1985.

Costalupes JA, Young ED, Gibson DJ (1984) Effects of continuous noise backgrounds on rate response of auditory nerve fibers in cat. J Neurophysiol. Jun;51(6):1326-44. doi: 10.1152/jn.1984.51.6.1326.

Creutzfeldt O, Hellweg FC, Schreiner C (1980) Thalamocortical transformation of responses to complex auditory stimuli. Exp Brain Res;39(1):87-104. doi: 10.1007/BF00237072.

Deneux T, Kempf A, Daret A, Ponsot E, Bathellier B (2016) Temporal asymmetries in auditory coding and perception reflect multi-layered nonlinearities. Nat Commun. Sep 1;7:12682. doi: 10.1038/ncomms12682.

Ding N, Melloni L, Yang A, Wang Y, Zhang W, Poeppel D (2017) Characterizing Neural Entrainment to Hierarchical Linguistic Units using Electroencephalography (EEG). Front Hum Neurosci. Sep 28;11:481. doi: 10.3389/fnhum.2017.00481.

Ding N, Chatterjee M, Simon JZ. (2014) Robust cortical entrainment to the speech envelope relies on the spectro-temporal fine structure. Neuroimage. Mar;88:41-6. doi: 10.1016/j.neuroimage.2013.10.054.

Drullman R, Festen JM, Plomp R (1994b) Effect of reducing slow temporal modulations on speech reception. J Acoust Soc Am. May;95(5 Pt 1):2670-80. doi: 10.1121/1.409836.

Drullman R, Festen JM & Plomp R (1994a) Effect of temporal envelope smearing on speech reception. The Journal of the Acoustical Society of America 95, 1053–1064.

Edeline JM, Manunta Y, Nodal F, Bajo V (1999) Do auditory responses recorded from awake animals reflect the anatomical parcellation of the auditory thalamus? Hearing Research, 131, 135-152.

Franke F, Quian Quiroga R, Hierlemann A, Obermayer K (2015) Bayes optimal template matching for spike sorting - combining fisher discriminant analysis with optimal filtering. J Comput Neurosci. 38(3):439-59.

Frisina RD, Karcich KJ, Tracy TC, Sullivan DM, Walton JP, Colombo J. (1996) Preservation of amplitude modulation coding in the presence of background noise by chinchilla auditory-nerve fibers. J Acoust Soc Am. Jan;99(1):475-90. doi: 10.1121/1.414559.

Frisina RD, Smith RL, Chamberlain SC (1990) Encoding of amplitude modulation in the gerbil cochlear nucleus: I. A hierarchy of enhancement. Hear. Res. 44, 99–122.

Gaucher Q, Edeline JM (2015) Stimulus-specific effects of noradrenaline in auditory cortex: implications for the discrimination of communication sounds. J. Physiol. (Lond.) 593, 1003–1020.

Gaucher Q, Edeline JM, Gourévitch B (2012) How different are the local field potentials and spiking activities? Insights from multi-electrodes arrays. J. Physiol. Paris 106, 93–103.

Gaucher Q, Huetz C, Gourévitch B, Edeline JM (2013a) Cortical inhibition reduces information redundancy at presentation of communication sounds in the primary auditory cortex. J. Neurosci. 33, 10713–10728.
Geisler CD, Sinex DG (1980) Responses of primary auditory fibers to combined noise and tonal stimuli. Hear Res. (4):317-34. doi: 10.1016/0378-5955(80)90026-x.
Gnansia D, Péan V, Meyer B, Lorenzi C (2009) Effects of spectral smearing and temporal fine structure degradation on speech masking release. J. Acoust. Soc. Am. 125, 4023–4033.
Gnansia D, Pressnitzer D, Péan V, Meyer B, Lorenzi C (2010) Intelligibility of interrupted and interleaved speech for normal-hearing listeners and cochlear implantees. Hearing Research 265, 46–53.
Gourévitch B, Edeline JM (2011) Age-related changes in the guinea pig auditory cortex: relationship with brainstem changes and comparison with tone-induced hearing loss. Eur. J. Neurosci. 34, 1953–1965.
Gourévitch B, Doisy T, Avillac M, Edeline JM (2009) Follow-up of latency and threshold shifts of auditory brainstem responses after single and interrupted acoustic trauma in guinea pig. Brain Res. 1304, 66–79.
Grimsley JM, Palmer AR, Wallace MN (2011) Different representations of tooth chatter and purr call in guinea pig auditory cortex. Neuroreport. Aug 24;22(12):613-6. doi: 10.1097/WNR.0b013e3283495ae9.
Grimsley JMS, Shanbhag SJ, Palmer AR, Wallace MN (2012) Processing of Communication Calls in Guinea Pig Auditory Cortex. PLoS ONE 7, e51646.
Harris KD (2020) Nonsense correlations in neuroscience. bioRxiv 2020.11.29.402719; doi: https://doi.org/10.1101/2020.11.29.402719.
Heil P, (2003) Coding of temporal onset envelope in the auditory system. Speech Commun. 41 (1), 123–134.
Hohmann V (2002) Frequency analysis and synthesis using a Gammatone filterbank. Acust Acta Acust 88:433–442.
Homma NY, Hullett PW, Atencio CA, Schreiner CE (2020) Auditory Cortical Plasticity Dependent on Environmental Noise Statistics. Cell Rep. Mar 31;30(13):4445-4458.e5. doi: 10.1016/j.celrep.2020.03.014.
Joris PX, Schreiner CE, Rees A (2004) Neural processing of amplitude-modulated sounds. Physiol. Rev. 84, 541–577.
Kates JM (2011) Spectro-temporal envelope changes caused by temporal fine structure modification. The Journal of the Acoustical Society of America 129, 3981–3990.
Kösem A & Van Wassenhove V (2017) Distinct contributions of low-and high-frequency neural oscillations to speech comprehension. Language, Cognition and Neuroscience, 32(5), 536-544.
Kösem A, Basirat A, Azizi L, & van Wassenhove V (2016) High-frequency neural activity predicts word parsing in ambiguous speech streams. Journal of neurophysiology, 116(6), 2497-2512.
Langner G, Schreiner CE (1988) Periodicity coding in the inferior colliculus of the cat. I. Neuronal mechanisms. J Neurophysiol. Dec;60(6):1799-822. doi: 10.1152/jn.1988.60.6.1799.
Langner G. (1992) Periodicity coding in the auditory system. Hear Res. 60(2):115-42. doi: 10.1016/0378-5955(92)90015-f.
Langner G, Dinse HR, Godde B (2009) A map of periodicity orthogonal to frequency representation in the cat auditory cortex. Front Integr Neurosci. 3:27. doi: 10.3389/neuro.07.027.2009.
Liang L, Lu T, Wang X. (2002) Neural representations of sinusoidal amplitude and frequency modulations in the primary auditory cortex of awake primates. J Neurophysiol. 87(5):2237-61. doi: 10.1152/jn.2002.87.5.2237.
Lu T, Liang L, Wang X. (2001a) Temporal and rate representations of time-varying signals in the auditory cortex of awake primates. Nat Neurosci.;4(11):1131-8. doi: 10.1038/nn737.
Lu T, Liang L, Wang X (2001b) Neural representations of temporally asymmetric stimuli in the auditory cortex of awake primates. J Neurophysiol. 85(6):2364-80. doi: 10.1152/jn.2001.85.6.2364.
Lu T, Wang X (2004) Information content of auditory cortical responses to time-varying acoustic stimuli. J Neurophysiol. 91(1):301-13. doi: 10.1152/jn.00022.2003.
Luo H, & Poeppel D (2007). Phase patterns of neuronal responses reliably discriminate speech in human auditory cortex. Neuron, 54(6), 1001–1010. doi:10.1016/j.neuron.2007.06.004
Majdak P, Hollomey C, and Baumgartner R (2022) AMT 1.0: the toolbox for reproducible research in auditory modeling. Acta Acustica.
Nagarajan SS et al. (2002) Representation of Spectral and Temporal Envelope of Twitter Vocalizations in Common Marmoset Primary Auditory Cortex. Journal of Neurophysiology 87, 1723–1737.
Narayan, R. et al. Cortical interference effects in the cocktail party problem. Nature Neuroscience 10, 1601–1607 (2007).
Neuert V, Pressnitzer D, Patterson RD, Winter IM (2001) The responses of single units in the inferior colliculus of the guinea pig to damped and ramped sinusoids. Hear Res. Sep;159(1-2):36-52. doi: 10.1016/s0378-5955(01)00318-5.

Nourski KV, Reale RA, Oya H, Kawasaki H, Kovach CK, Chen H, Howard MA 3rd, Brugge JF (2009) Temporal envelope of time-compressed speech represented in the human auditory cortex. J Neurosci. Dec 9;29(49):15564-74. doi: 10.1523/JNEUROSCI.3065-09.2009.

Occelli F, Suied C, Pressnitzer D, Edeline JM, Gourévitch B (2016) A Neural Substrate for Rapid Timbre Recognition? Neural and Behavioral Discrimination of Very Brief Acoustic Vowels. Cereb. Cortex 26, 2483–2496.

Ortiz Barajas MC, Guevara R, Gervain J (2021) The origins and development of speech envelope tracking during the first months of life. Dev Cogn Neurosci. Apr;48:100915. doi: 10.1016/j.dcn.2021.100915.

Osses Vecchi A, Varnet L, Carney LH., Dau T, Bruce IC, Verhulst S, and Majdak P (2022) A comparative study of eight human auditory models of monaural processing. Acta Acustica. 6, 17.

Palmer AR, Evans EF (1982) Intensity coding in the auditory periphery of the cat: responses of cochlear nerve and cochlear nucleus neurons to signals in the presence of bandstop masking noise. Hear Res. Aug;7(3):305-23. doi: 10.1016/0378-5955(82)90042-9.

Paraouty N, Stasiak A, Lorenzi C, Varnet L, Winter IM (2018) Dual Coding of Frequency Modulation in the Ventral Cochlear Nucleus. J. Neurosci. 38, 4123–4137.

Patterson RD (1987) A pulse ribbon model of monaural phase perception. J. Acoust. Soc. Am. 82, 1560–1586.

Pefkou M, Arnal LH, Fontolan L, Giraud AL. (2017) θ-Band and β-Band Neural Activity Reflects Independent Syllable Tracking and Comprehension of Time-Compressed Speech. J Neurosci. Aug 16;37(33):7930-7938. doi: 10.1523/JNEUROSCI.2882-16.2017.

Philibert B, Laudanski J, Edeline JM (2005) Auditory thalamus responses to guinea-pig vocalizations: a comparison between rat and guinea-pig. Hear Res. Nov;209(1-2):97-103. doi: 10.1016/j.heares.2005.07.004.

Pouzat C, Delescluse M, Viot P, Diebolt J (2004) Improved spike-sorting by modeling firing statistics and burst-dependent spike amplitude attenuation: a Markov chain Monte Carlo approach. J Neurophysiol. 91(6):2910-28.

Quiroga RQ, Nadasdy Z, Ben-Shaul Y (2004) Unsupervised spike detection and sorting with wavelets and superparamagnetic clustering. Neural Comput. 16(8):1661-87.

Rabinowitz NC, Willmore BD, King AJ, Schnupp JW (2013) Constructing noise-invariant representations of sound in the auditory pathway. PLoS Biol. Nov;11(11):e1001710. doi: 10.1371/journal.pbio.1001710.

Ramachandran R, Davis KA, May BJ (2000) Rate representation of tones in noise in the inferior colliculus of decerebrate cats. J Assoc Res Otolaryngol. 1(2):144-60. doi: 10.1007/s101620010029.

Ranasinghe KG, Vrana WA, Matney CJ, Kilgard MP (2012b) Neural Mechanisms Supporting Robust Discrimination of Spectrally and Temporally Degraded Speech. Journal of the Association for Research in Otolaryngology 13, 527–542.

Ranasinghe KG, Carraway RS, Borland MS, Moreno NA, Hanacik EA, Miller RS, Kilgard MP (2012a) Speech discrimination after early exposure to pulsed-noise or speech. Hear Res. Jul;289(1-2):1-12. doi: 10.1016/j.heares.2012.04.020.

Redies H, Brandner S, Creutzfeldt OD (1989) Anatomy of the auditory thalamocortical system of the guinea pig. The Journal of Comparative Neurology 282, 489–511.

Reiss LA, Ramachandran R, May BJ (2011) Effects of signal level and background noise on spectral representations in the auditory nerve of the domestic cat. J Assoc Res Otolaryngol. 12(1):71-88. doi: 10.1007/s10162-010-0232-5.

Rhode WS, Greenberg S (1994b) Encoding of amplitude modulation in the cochlear nucleus of the cat. J. Neurophysiol. 71, 1797–1825.

Rhode WS, Geisler CD, Kennedy DT (1978) Auditory nerve fiber response to wide-band noise and tone combinations. J Neurophysiol. May;41(3):692-704. doi: 10.1152/jn.1978.41.3.692.

Rode T, Hartmann T, Hubka P, Scheper V, Lenarz M, Lenarz T, Kral A, Lim HH (2013) Neural representation in the auditory midbrain of the envelope of vocalizations based on a peripheral ear model. Front Neural Circuits. Oct 21;7:166. doi: 10.3389/fncir.2013.00166.

Rosen S (1992) Temporal information in speech: acoustic, auditory and linguistic aspects. Philos Trans R Soc Lond B Biol Sci. Jun 29;336(1278):367-73. doi: 10.1098/rstb.1992.0070.

Rutkowski RG, Shackleton TM, Schnupp JWH, Wallace MN, Palmer AR (2002) Spectrotemporal Receptive Field Properties of Single Units in the Primary, Dorsocaudal and Ventrorostral Auditory Cortex of the Guinea Pig. Audiology and Neurotology 7, 214–227.

Sayles M, Winter IM (2010) Equivalent-rectangular bandwidth of single units in the anaesthetized guinea-pig ventral cochlear nucleus. Hear. Res. 262, 26–33.

Shamma S, Lorenzi C (2013) On the balance of envelope and temporal fine structure in the encoding of speech in the early auditory system. J Acoust Soc Am. May;133(5):2818-33. doi: 10.1121/1.4795783.

Shannon RV, Zeng FG, Kamath V, Wygonski J & Ekelid M (1995) Speech Recognition with Primarily Temporal Cues. Science 270, 303–304.

Shetake JA, Wolf JT, Cheung RJ, Engineer CT, Ram SK, Kilgard MP (2011) Cortical activity patterns predict robust speech discrimination ability in noise. Eur J Neurosci. Dec;34(11):1823-38. doi: 10.1111/j.1460-9568.2011.07887.x.

Schreiner CE, Langner G (1988) Periodicity coding in the inferior colliculus of the cat. II. Topographical organization. J Neurophysiol. 60(6):1823-40. doi: 10.1152/jn.1988.60.6.1823.

Schnupp JW, Garcia-Lazaro JA, Lesica NA (2015) Periodotopy in the gerbil inferior colliculus: local clustering rather than a gradient map. Front Neural Circuits.;9:37. doi: 10.3389/fncir.2015.00037.

Schnupp JWH, Hall TM, Kokelaar RF, Ahmed B (2006) Plasticity of temporal pattern codes for vocalization stimuli in primary auditory cortex. J. Neurosci. 26, 4785–4795.

Souffi S, Lorenzi C, Huetz C, Edeline JM (2021) Robustness to Noise in the Auditory System: A Distributed and Predictable Property. eNeuro. Mar 18;8(2):ENEURO.0043-21.2021. doi: 10.1523/ENEURO.0043-21.2021.

Souffi S, Lorenzi C, Varnet L, Huetz C, Edeline JM (2020) Noise-Sensitive But More Precise Subcortical Representations Coexist with Robust Cortical Encoding of Natural Vocalizations. J Neurosci. Jul 1;40(27):5228-5246. doi: 10.1523/JNEUROSCI.2731-19.2020..

Stone MA, Füllgrabe C, Mackinnon RC, Moore BCJ (2011) The importance for speech intelligibility of random fluctuations in 'steady' background noise. J. Acoust. Soc. Am. 130, 2874–2881.

Suta D, Popelár J, Kvasnák E, Syka J (2007) Representation of species-specific vocalizations in the medial geniculate body of the guinea pig. Exp Brain Res. Nov;183(3):377-88. doi: 10.1007/s00221-007-1056-3.

Suta D, Kvasnák E, Popelár J, Syka J (2003) Representation of species-specific vocalizations in the inferior colliculus of the guinea pig. J Neurophysiol. Dec;90(6):3794-808. doi: 10.1152/jn.01175.2002.

Tanaka H, Taniguchi I (1991) Responses of medial geniculate neurons to species-specific vocalized sounds in the guinea pig. Jpn J Physiol.41(6):817-29. doi: 10.2170/jjphysiol.41.817.

Ter-Mikaelian M, Semple MN, Sanes DH (2013) Effects of spectral and temporal disruption on cortical encoding of gerbil vocalizations. Journal of Neurophysiology 110, 1190–1204.

Varnet L, Ortiz-Barajas MC, Erra RG, Gervain J, Lorenzi C (2017) A cross-linguistic study of speech modulation spectra. The Journal of the Acoustical Society of America 142, 1976–1989.

Walker KM, Ahmed B, Schnupp JW (2008) Linking cortical spike pattern codes to auditory perception. J Cogn Neurosci. Jan;20(1):135-52. doi: 10.1162/jocn.2008.20012.

Wallace MN, Palmer AR (2008) Laminar differences in the response properties of cells in the primary auditory cortex. Exp Brain Res 184, 179–191.

Wallace MN, Shackleton TM, Anderson LA, Palmer AR (2005) Representation of the purr call in the guinea pig primary auditory cortex. Hear Res. Jun;204(1-2):115-26. doi: 10.1016/j.heares.2005.01.007.

Wallace MN, Rutkowski RG, Palmer AR (2000) Identification and localisation of auditory areas in guinea pig cortex. Experimental Brain Research 132, 445–456.

Wallace MN, Palmer AR (2009) Functional subdivisions in low-frequency primary auditory cortex (AI) Exp Brain Res. Apr;194(3):395-408. doi: 10.1007/s00221-009-1714-8.

Wallace MN, Anderson LA, Palmer AR (2007) Phase-Locked Responses to Pure Tones in the Auditory Thalamus. Journal of Neurophysiology 98, 1941–1952.

Wang X, Merzenich MM, Beitel R, Schreiner CE (1995) Representation of a species-specific vocalization in the primary auditory cortex of the common marmoset: temporal and spectral characteristics. Journal of Neurophysiology 74, 2685–2706.

Woolley SM, Gill PR, Theunissen FE (2006) Stimulus-dependent auditory tuning results in synchronous population coding of vocalizations in the songbird midbrain. J Neurosci. Mar 1;26(9):2499-512. doi: 10.1523/JNEUROSCI.3731-05.2006.

Young ED, Barta PE (1986) Rate responses of auditory nerve fibers to tones in noise near masked threshold. J Acoust Soc Am. Feb;79(2):426-42. doi: 10.1121/1.393530.

Zeng FG, Nie K, Stickney GS, Kong YY, Vongphoe M, Bhargave A, Wei C, Cao K. (2005) Speech recognition with amplitude and frequency modulations. Proc. Natl. Acad. Sci. USA, 102, 2293-2298.

Zoefel B, VanRullen R (2016) EEG oscillations entrain their phase to high-level features of speech sound. Neuroimage. Jan 1;124(Pt A):16-23. doi: 10.1016/j.neuroimage.2015.08.054.

Additional information section

Data availability statement

The data that support the findings of this study are available from the corresponding author upon reasonable request.

Competing interests

The authors declare no competing financial interests.

Author contributions

This work was performed at the Paris-Saclay Institute of Neurosciences (NeuroPSI). S.S. and J-M.E. designed the experiments. S.S. and M.Z. performed the experiments. S.S., L.V., B.B. and C.H. have participated in the acquisition, analysis or interpretation of data. All authors drafting the work or revising it critically for important intellectual content. All authors approved the final version of the manuscript. All authors agree to be accountable for all aspects of the work in ensuring that questions related to the accuracy or integrity of any part of the work are appropriately investigated and resolved; and all persons designated as authors qualify for authorship, and all those who qualify for authorship are listed.

Funding

JME was supported by grants from the French Agence Nationale de la Recherche (ANR) (ANR-14-CE30-0019-01). SS was supported by the Fondation pour la Recherche Médicale (FRM) grant number ECO20160736099 and by the Entendre Foundation.

Acknowledgements

We thank Nihaad Paraouty for training us on the cochlear nucleus surgery. We thank Prf. Christian Lorenzi and Prf. Shihab Shamma for helpful comments on a previous version of the MS, and are particularly grateful to Dr. Virginie van Wassenhove for suggesting several improvements of the MS. We also wish to thank Céline Dubois, Mélanie Dumont and Aurélie Bonilla, for taking care of the guinea-pig colony.

Figure legends

Figure 1. Overall and filtered envelopes in three amplitude modulation ranges.
A. Spectrograms of original and degraded stimuli.
B. Overall envelopes of original and degraded stimuli. The envelopes of the four original whistles are presented on the left panel. Two whistles were used for a Go/No-Go behavioral discrimination task (see Fig. 7D): whistle 1 as the "Go or S+" stimulus and whistle 3 as the "No-Go or S-" stimulus. From left to right, the four envelopes of these stimuli are presented first, in the vocoding conditions (with 38, 20 and 10 frequency bands from top to bottom), then in stationary noise (at +10, 0 and -10 dB SNR from top to bottom) and in chorus noise conditions (at +10, 0 and -10 dB SNR from top to bottom).
C. Examples of the filtered envelopes for the original vocalizations using a bank of 35 gammatone filters with center frequencies uniformly spaced along a guinea pig - adapted ERB (equivalent rectangular bandwidth) scale ranging from 20 to 30 000 Hz. Three ranges of amplitude modulation (AM) have been investigated here: the low (<20 Hz), middle (between 20 and 100 Hz) and high (between 100 and 200 Hz) AM ranges. The red curves indicate the seven filtered envelopes selected along the signal for the subsequent analyses.

Figure 2. Correlations in the original condition between peri-stimulus time histograms (PSTHs) of subcortical and cortical recordings and the stimulus envelope both filtered in the three selected AM ranges.
A. Individual examples of original PSTHs obtained in each structure (from bottom to top, sANF: simulated auditory nerve fibers, CN: cochlear nucleus, CNIC: central nucleus of the inferior colliculus, MGv: ventral division of the medial geniculate, A1: primary auditory cortex, VRB: ventro-rostral belt).
B. Population responses ranked from the lowest to the highest best frequencies with the color code representing the normalized firing rate. On the bottom of each panel, the population firing rate represents the instantaneous summed activity of the whole virtual population, and on the right, the total firing rate along the different best frequencies.
C-E. Examples of correlations between the PSTH (in black) and the envelope (in red). In each panel, the PSTHs and the stimulus envelopes are filtered in the same frequency range. For each recording, the correlation value between the PSTH and the envelope is shown on the top left. In a given AM range, the stimulus envelopes differ between examples because we selected the gammatone envelope (out of seven gammatones) which induced the highest correlation. Note that the PSTHs are not lagged compared to the envelopes as during the analysis.
F. Box plots showing the distributions of the $Rmax_{E\text{-}PSTH}$ values for the six auditory structures (sANF to VRB) in the three AM ranges. The red dots in the box plots correspond to the mean $Rmax_{E\text{-}PSTH}$ values and the boxes correspond to the interquartile ranges. Note the higher $Rmax_{E\text{-}PSTH}$ values in the low (L) AM range compared with the middle (M) and high (H) AM ranges. The black lines represent significant differences between the mean $Rmax_{E\text{-}PSTH}$ values. In the low AM range, sANF, CN and CNIC recordings displayed significantly higher mean $Rmax_{E\text{-}PSTH}$ values than MGv and cortical recordings (low AM range: one-way ANOVA, $p < 0.0001$ $F_{(5,\ 1165)} = 138.25$ with Students' t test unpaired, sANF vs. MGv, A1 or VRB $p<0.0001$, CN vs. MGv, A1 or VRB $p<0.0001$, CNIC vs. MGv, A1 or VRB $p<0.0001$; mean (± STD) $Rmax_{E\text{-}PSTH}$ values: $R_{sANF(n = 217)}$= 0.81 ± 0.03, $R_{CN(n = 336)}$= 0.80 ± 0.08, $R_{CNIC(n = 274)}$= 0.78 ± 0.11, $R_{MGv(n = 102)}$= 0.68 ± 0.13, $R_{A1(n = 171)}$= 0.60 ± 0.13 and $R_{VRB(n = 66)}$= 0.63 ± 0.14). In the middle and high AM ranges, the CNIC recordings still exhibited slightly higher mean $Rmax_{E\text{-}PSTH}$ values compared to the other structures (mean (± STD) $Rmax_{E\text{-}PSTH}$ values in the middle AM range: $R_{sANF(n = 44)}$= 0.32 ± 0.03, $R_{CN(n = 285)}$= 0.31 ± 0.07, $R_{CNIC(n = 285)}$= 0.34 ± 0.07, $R_{MGv(n = 133)}$= 0.31 ± 0.07, $R_{A1(n = 220)}$= 0.27 ± 0.05 and $R_{VRB(n =85)}$= 0.29 ± 0.06; mean (± STD) $Rmax_{E\text{-}PSTH}$ values in the high AM range: $R_{sANF(n = 77)}$= 0.31 ± 0.03, $R_{CN(n = 249)}$= 0.31 ± 0.05, $R_{CNIC(n =257)}$= 0.33 ± 0.05, $R_{MGv(n = 97)}$= 0.29 ± 0.04, $R_{A1(n = 196)}$= 0.27 ± 0.05

and $R_{VRB(n=50)}$= 0.30 ± 0.05). Note that n values correspond to the selected simulations or recordings.

Figure 3. In the original condition, the better cortical and subcortical neurons track the slow envelope (<20 Hz), the higher the value of mutual information.

A. Box plots showing the distributions of the MI values obtained in the six levels of the auditory system in the original condition. The red dots in the box plots correspond to the mean MI values and the boxes correspond to the interquartile ranges. Note the lower significant values obtained at the cortical level in AI and VRB compared to those obtained in sANF and subcortical structure (one-way ANOVA $p < 0.0001$ $F_{(5, 1538)} = 266.46$ with Students' t test unpaired, sANF vs. A1 or VRB p<0.0001, CN vs. A1 or VRB $p < 0.0001$, CNIC vs. A1 or VRB $p < 0.0001$, MGv vs. A1 or VRB $p < 0.0001$; mean (± STD) MI values: $MI_{sANF(n=77)}$= 1.84 ± 0.21 bits, $MI_{CN(n=249)}$= 0.92 ± 0.47 bits, $MI_{CNIC(n=257)}$= 1 ± 0.5 bits, $MI_{MGv(n=97)}$= 1.19 ± 0.55 bits, $MI_{A1(n=196)}$= 0.68 ± 0.37 bits and $R_{VRB(n=50)}$= 0.55 ± 0.29 bits). Note that n values correspond to the selected simulations or recordings. The black lines represent the first significant differences between the mean values. Note that for the sake of clarity, not all significant differences are indicated by black lines. For example, the difference between sANF and MGv was the first one to be significant but it was also significant between sANF and the two cortical areas A1 and VRB.

B. Scattergrams showing the relationships between $Rmax_{E\text{-}PSTH}$ and MI values for the six structures in the three AM ranges. Black lines correspond to the linear regression lines.

C. Matrix summarizing the correlation coefficients between $Rmax_{E\text{-}PSTH}$ and MI in each structure and AM range. The values in red indicate that the correlation was significant. In all but one case (in CNIC in the middle AM range), significant positive correlations between $Rmax_{E\text{-}PSTH}$ and MI values were obtained in all AM ranges in subcortical structures ($p^L_{CN} < 0.0001$, $p^M_{CN} < 0.0001$, $p^H_{CN} = 0.01$, $p^L_{CNIC} < 0.0001$, $p^M_{CNIC} = 0.24$, $p^H_{CNIC} = 0.005$, $p^L_{MGv} = 0.006$, $p^M_{MGv} < 0.0001$, $p^H_{MGv} = 0.01$). For the sANF, the range of MI values was too limited to compute reliable correlations (most MI values were close to the maximum of 2 bits). At the subcortical level, the highest correlation values between $Rmax_{E\text{-}PSTH}$ and MI values were found in MGv. At the cortical level, significant correlations between $Rmax_{E\text{-}PSTH}$ and MI values were detected in the low and middle AM ranges in A1 ($p^L_{A1} = 0.01$, $p^M_{A1} = 0.05$, $p^H_{A1} = 0.32$) and there was no significant correlation in VRB ($p^L_{VRB} = 0.31$, $p^M_{VRB} = 0.51$, $p^H_{VRB} = 0.99$).

Figure 4. Neuronal discrimination performance in all degraded conditions along the auditory system.

A-F. Neuronal discrimination performance (quantified by the mutual information, in bits) in original condition and in the three situations of acoustic degradation (top panels: vocoding, middle panels: stationary noise and bottom panels: chorus noise). In each box plot, the horizontal line corresponds to the median value and the boxes correspond to the interquartile ranges. For all structures except in sANF, note the largest decrease in MI value in the stationary noise in the subcortical structures compared with the relative stability of these values in vocoding and chorus noise. Note also the much smaller decreases observed at the cortical level in the three situations of acoustic alterations. The stars represent the first significant differences between the mean original values and those obtained in degraded conditions. Note that for the sake of clarity, not all significant differences are indicated by stars. The decrease was significant only for the 10-band vocoded vocalizations in MGv and A1 (Fig. 4D, one-way ANOVA, $p = 0.05$ $F_{(3, 811)} = 2.58$ with Students' t test paired, MGv_{Ori} vs. MGv_{Voc10} $p < 0.0001$; Fig. 4E, one-way ANOVA, $p = 0.001$ $F_{(3, 722)} = 3.73$ with Students' t test paired, $A1_{Ori}$ vs. $A1_{Voc10}$ $p < 0.0001$), and no significant difference was detected in VRB (Fig.4F, one-way ANOVA, $p = 0.75$ $F_{(3, 186)} = 0.41$). The decrease was already significant with 38-band vocoded vocalizations in sANF or with 20-band vocoded vocalizations in CN and CNIC (Fig. 4A, one-way ANOVA, $p < 0.0001$ $F_{(3, 1302)} = 111.3$ with Students' t test paired, $sANF_{Ori}$ vs. $sANF_{Voc38}$ $p < 0.0001$; Fig.4B, one-way ANOVA, $p < 0.0001$ $F_{(3, 1424)} = 12.42$ with Students' t test paired, CN_{Ori} vs. CN_{Voc20} $p < 0.0001$; Fig. 4C, one-way ANOVA, $p < 0.0001$ $F_{(3,}$

$_{1231)}$ = 13.17 with Students' t test paired, $CNIC_{Ori}$ vs. $CNIC_{Voc20}$ $p < 0.0001$). Note that there was also a significant increase in MI values with the 38-band vocoded vocalizations in CN (Fig.4B, one-way ANOVA, $p < 0.0001$ $F_{(3, 1424)} = 12.42$ with Students' t test paired, CN_{Ori} vs. CN_{Voc38} $p= 0.0073$). In chorus noise, in CN and CNIC, there was no significant decrease in mean MI values (Fig. 4B, one-way ANOVA, $p = 0.05$ $F_{(3, 1176)} = 2.65$; Fig. 4C, one-way ANOVA, $p = 0.36$ $F_{(3, 1188)} = 1.06$), whereas in sANF and MGv, the mean MI values significantly decreased at +10 dB or 0 dB SNR respectively (Fig. 4A, one-way ANOVA, $p < 0.0001$ $F_{(3, 1331)} = 232.86$ with Students' t test paired, $sANF_{Ori}$ vs. $sANF_{+10dB}$ $p < 0.0001$; Fig. 4D, one-way ANOVA, $p < 0.0001$ $F_{(3, 753)} = 7.3$ with Students' t test paired, MGv_{Ori} vs. MGv_{0dB} $p < 0.0001$). At the cortical level, there was a significant decrease in A1 at 0 dB SNR and no significant change of mean MI values in VRB (Fig. 4E, one-way ANOVA, $p = 0.0039$ $F_{(3, 697)} = 4.5$ with Students' t test paired, $A1_{Ori}$ vs. $A1_{0dB}$ $p < 0.0001$; Fig.4F, one-way ANOVA, $p = 0.31$ $F_{(3, 179)} = 1.19$). In stationary noise, the mean MI value in sANF, CN and MGv was significantly reduced already at +10 dB SNR (Fig. 4A, one-way ANOVA, $p < 0.0001$ $F_{(3, 1153)} = 767.64$ with Students' t test paired, $sANF_{Ori}$ vs. $sANF_{+10dB}$ $p < 0.0001$; Fig. 4B, one-way ANOVA, $p < 0.0001$ $F_{(3, 812)} = 61.22$ with Students' t test paired, CN_{Ori} vs. CN_{+10dB} $p < 0.0001$; Fig. 4D, one-way ANOVA, $p < 0.0001$ $F_{(3, 630)} = 62.03$ with Students' t test paired, MGv_{Ori} vs. MGv_{+10dB} $p < 0.0001$), whereas the mean MI value in CNIC was significantly reduced at 0 dB SNR (Fig. 4C, one-way ANOVA, $p < 0.0001$ $F_{(3, 1078)} = 32.08$ with Students' t test paired, $CNIC_{Ori}$ vs. $CNIC_{0dB}$ $p < 0.0001$). At the cortical level, stationary noise significantly reduced the mean MI value in A1 only at -10 dB SNR (Fig. 4E, one-way ANOVA, $p < 0.0001$ $F_{(3, 669)} = 13.99$ with Students' t test paired, $A1_{Ori}$ vs. $A1_{-10dB}$ $p < 0.0001$), whereas the mean MI values in VRB remained unchanged in all conditions (Fig. 4F, one-way ANOVA, $p = 0.26$ $F_{(3, 164)} = 1.34$).

Figure 5. Individual examples of correlations between neuronal responses and envelopes in all acoustic conditions and all structures.

Note that for the subcortical and cortical structures, we presented the results from the low AM range. The correlation value between the PSTH (in black) and the envelope (in red) is shown on the left. In all structures, the correlation values for these individual recordings remained similar between the acoustic conditions.

Figure 6. The envelope tracking is only slightly affected by the different situations of acoustic degradation.

Mean changes of the $Rmax_{E\text{-}PSTH}$ (±STD) quantified from the original condition in the different situations of acoustic degradations (vocoding, stationary noise (SN) and chorus noise (CN)) for all recordings obtained in the six structures. Note that, in each structure and AM range, the $Rmax_{E\text{-}PSTH}$ values were only slightly changed between the original and the degraded conditions. In sANF and CN, we observed a maximal increase in mean (± STD) $Rmax_{E\text{-}PSTH}$ values of 0.16 (±0.03) (and 0.11 (±0.13) for CN) and, a maximal decrease of 0.10 (±0.04) (and 0.05 (±0.06) for CN) depending on the degraded conditions and the AM range (Fig. 6). In CNIC and MGv, the mean (± STD) $Rmax_{E\text{-}PSTH}$ changes in degraded conditions were very small (Fig. 6, between -0.06 (±0.03) and 0.006 (±0.06) for CNIC and between -0.08 (±0.08) and -0.0002 (±0.15) for MGv). In A1, the changes in mean (± STD) $Rmax_{E\text{-}PSTH}$ values varied between -0.09 (±0.11) and 0.07 (±0.15) and in VRB it varied between -0.13 (±0.13) and 0.07 (± 0.15).

Figure 7. In all situations of acoustic alteration, the decrease in neuronal discrimination performance can be explained by the increase in envelope similarity in the low range.

A. Acoustic similarity (R_{Env}) between the envelopes of the four whistles in the original condition (Ori) and in the three situations of acoustic alterations (vocoding, stationary noise and chorus noise) for the low (L, red lines), middle (M, yellow lines) and high (H, purple lines) AM ranges. Dark lines correspond to the R_{Env} values based on the 7 selected gammatones, whereas the light lines

correspond to the R_{Env} values based on the 35 gammatones. Note that in the stationary noise, the correlation between the stimulus envelopes largely increased in the L range, indicating that the stimuli tended to be similar to each other in these AM ranges, which was not the case in the middle and high ranges (M and H). This between-stimuli increase in correlation in the L range was much weaker in the vocoding and chorus noise situations.

B. Scattergrams showing the variation of the maximal correlation ($\Delta Rmax_{E\text{-}PSTH}$) in the low AM range as a function of the variation of MI (ΔMI) in the -10 dB SNR condition compared to the original condition in each structure.

C. Mean changes (ΔMI, in percentage) of mutual information in sANF, CN, CNIC MGv, A1 and VRB as a function of the variation (ΔR_{Env}, in percentage) of the acoustic similarity in low AM range relative to the original condition. Each dot represents neuronal data (ΔMI) in sANF (in dark red), CN (in black), CNIC (in green), MGv (in orange), A1 (in blue) and VRB (in purple). From left to right, all degraded acoustic conditions were organized according to the acoustic distance of the envelopes (R_{Env}) between the four whistles quantified on Figure 7A (+10 dB SNR - Chorus N., Voc 38, Voc20, +10 dB SNR - Stationary N., 0 dB SNR - Chorus N., Voc10, -10 dB SNR - Chorus N., 0 dB SNR - Stationary N., -10 dB SNR - Stationary N.). Linear fits were generated for the different structures across all degraded conditions (color lines). For the sake of clarity, we did not use an orthonormal coordinate system.

D. Percentage of correct responses obtained during the four last sessions for each condition. The dark thick line corresponds to the mean (±STD) values obtained for all mice. The individual performances of each mouse (n=9) are presented by the grey thin lines. The last four sessions of discrimination in the original conditions are represented followed by the discrimination in the three conditions in stationary noise (+10, 0 and -10 dB SNR), followed by the discrimination in the three conditions in chorus noise (+10, 0 and -10 dB SNR). The chance level is represented by the red dashed line. The drops in performance were observed for the 0 dB and the -10 dB SNR in the stationary noise. The inset shows that the decrease in behavioral performance (average across sessions and animals) was strongly related to the reduction in the differences between the two temporal envelopes (W1 and W3) in the low AM range.

Abstract figure legend

Methods: We simulated auditory nerve fiber (sANF) responses and recorded the neuronal activity in five auditory structures (from cochlear nucleus to secondary auditory cortex) in response to four vocalizations presented in quiet and in two types of noise (a stationary and a chorus noise at three SNRs: +10, 0 and -10 dB). In addition, we tested whether behaving animals can discriminate between whistles when engaged in a Go/No-Go task involving the discrimination between two of the four whistles used in our electrophysiological studies (W1 and W3). Licks to the S+ were rewarded by a drop of water and licks to the S- were punished by a 5-second time-out period.

Results: Subcortical and cortical auditory neurons track the slow changes of the temporal envelope (<20Hz), with a high degree of fidelity in the original (positively correlated with the neuronal discrimination) and degraded conditions. Our results demonstrate that the between-stimulus envelope similarity, which increases in noise, negatively correlates both with the neuronal discrimination and the behavioral performance.

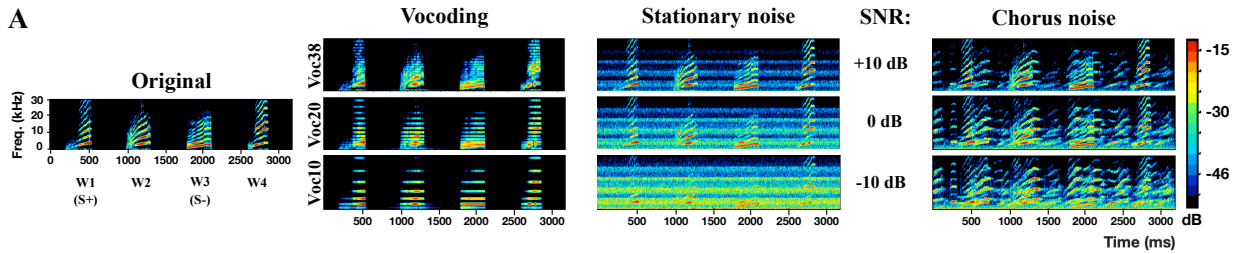
A
Original
Vocoding
Stationary noise
SNR:
Chorus noise
Freq. (kHz)
W1
(S+)
W2
W3
(S-)
W4
Voc38
Voc20
Voc10
+10 dB
0 dB
-10 dB
-15
-30
-46
dB
Time (ms)

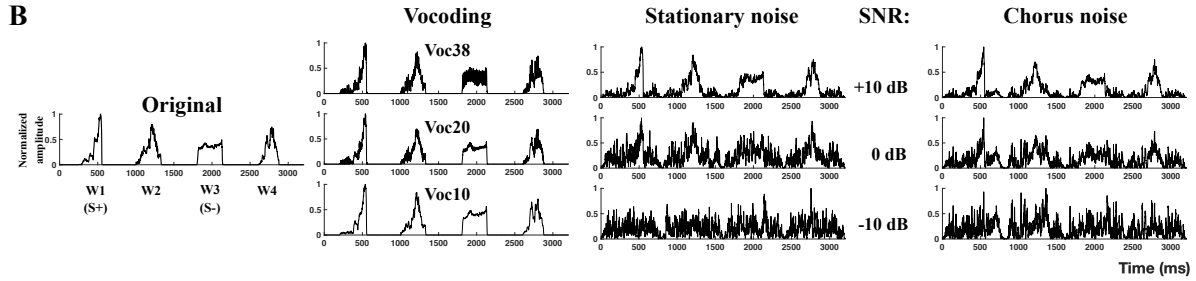
B
Original
Vocoding
Stationary noise
SNR:
Chorus noise
Normalized amplitude
W1
(S+)
W2
W3
(S-)
W4
Voc38
Voc20
Voc10
+10 dB
0 dB
-10 dB
Time (ms)

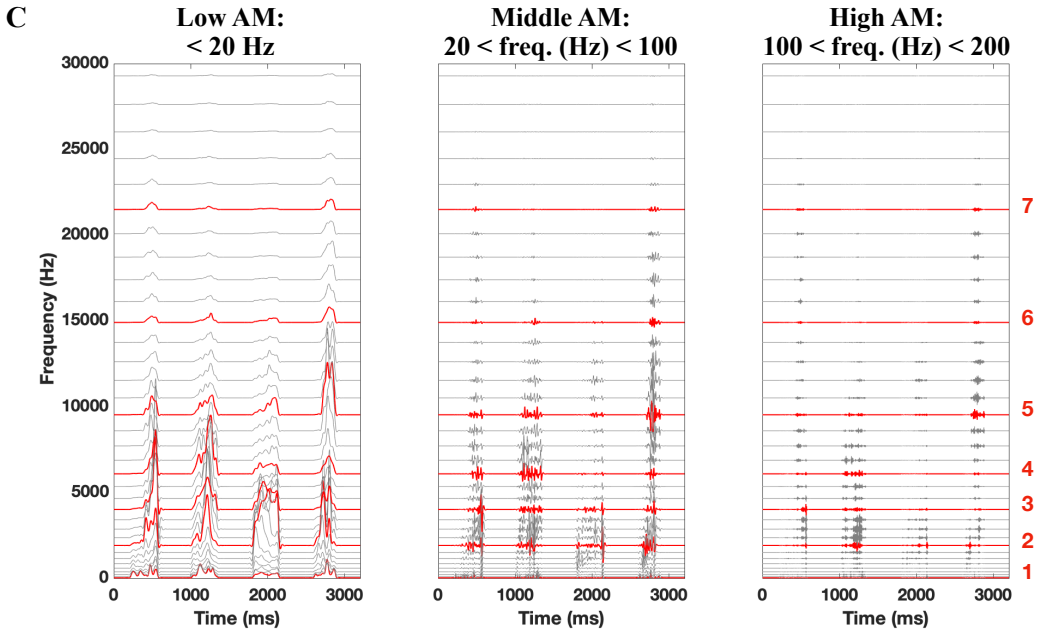
C
Low AM:
< 20 Hz
Middle AM:
20 < freq. (Hz) < 100
High AM:
100 < freq. (Hz) < 200
Frequency (Hz)
Time (ms)
7
6
5
4
3
2
1

Figure 1.

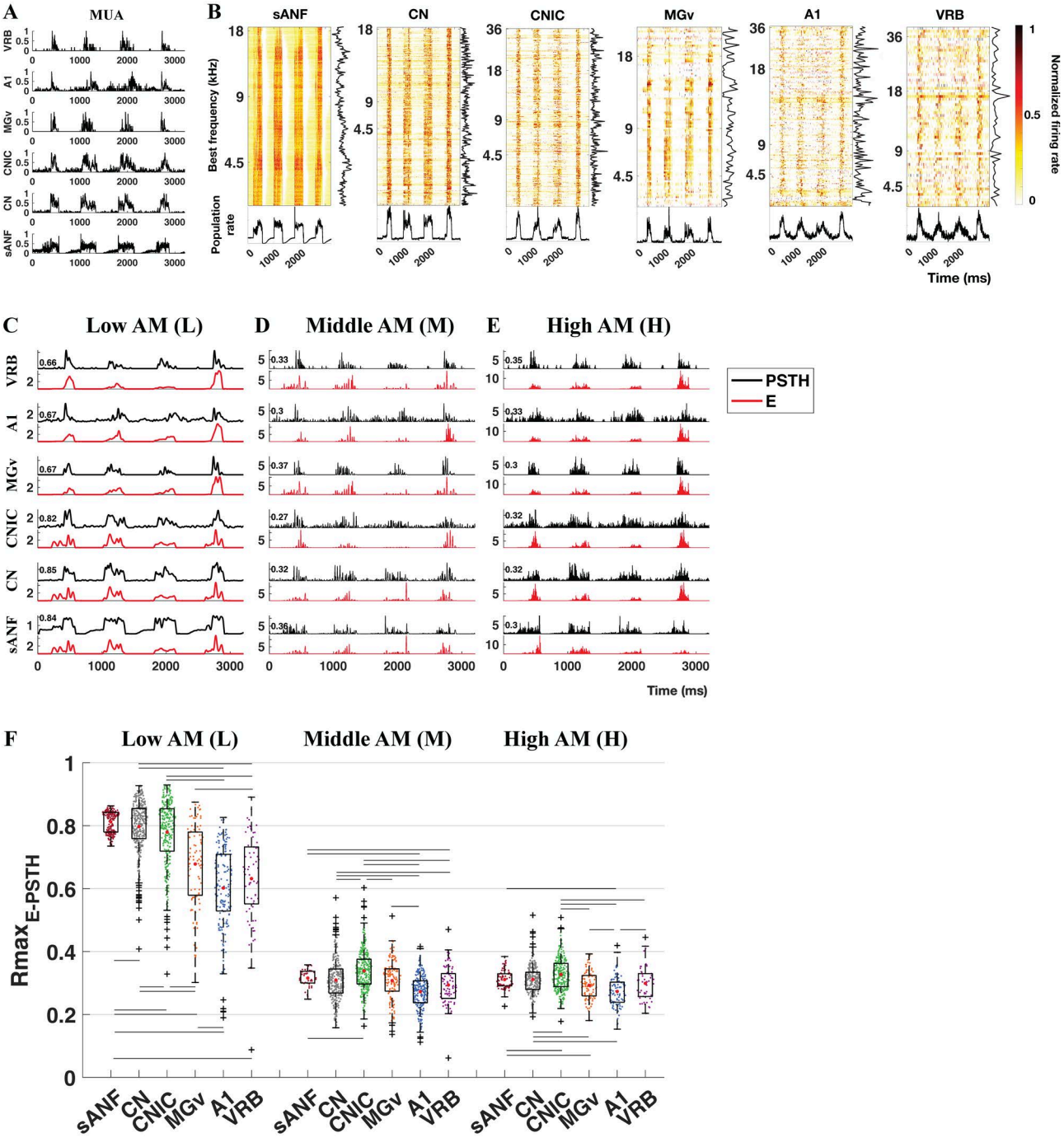
A
MUA
VRB
A1
MGv
CNIC
CN
sANF
B
sANF
CN
CNIC
MGv
A1
VRB
Best frequency (kHz)
Population rate
Normalized firing rate
Time (ms)
C
Low AM (L)
D
Middle AM (M)
E
High AM (H)
PSTH
E
Time (ms)
F
Low AM (L)
Middle AM (M)
High AM (H)
Rmax E-PSTH

Figure 2.

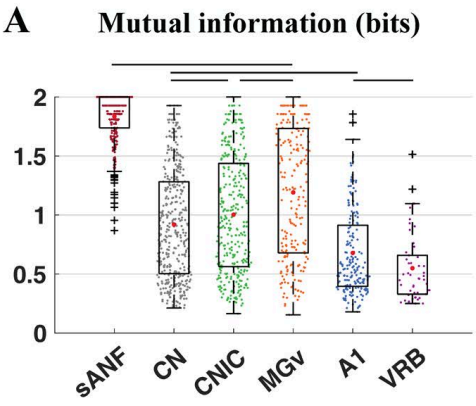

C Correlation values between Rmax E-PSTH and MI

	L	M	H
VRB	0.19	0.10	0.00
A1	0.27	0.19	0.14
MGv	0.29	0.42	0.27
CNIC	0.30	0.07	0.18
CN	0.29	0.35	0.17

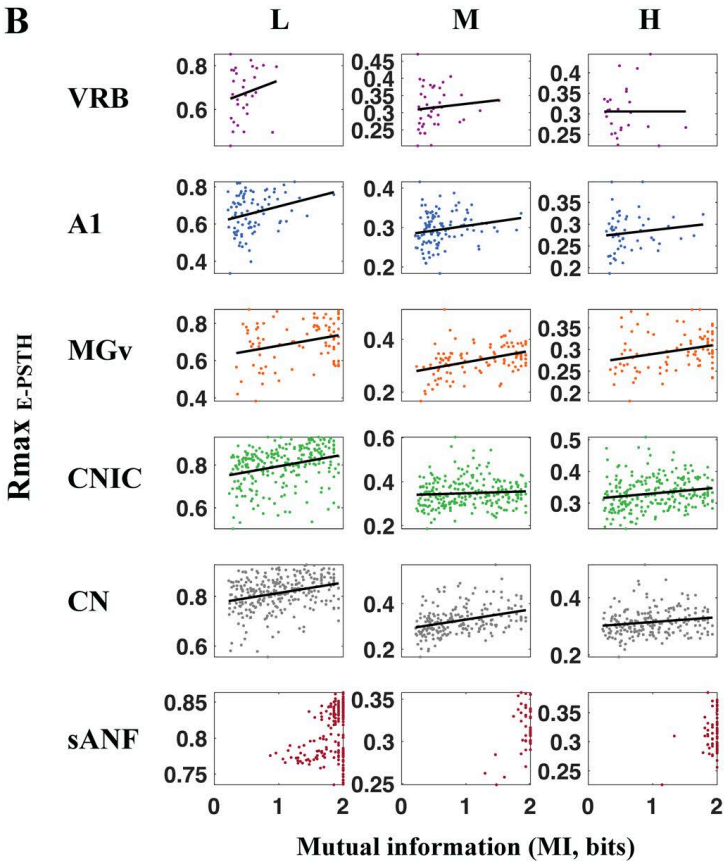

Figure 3.

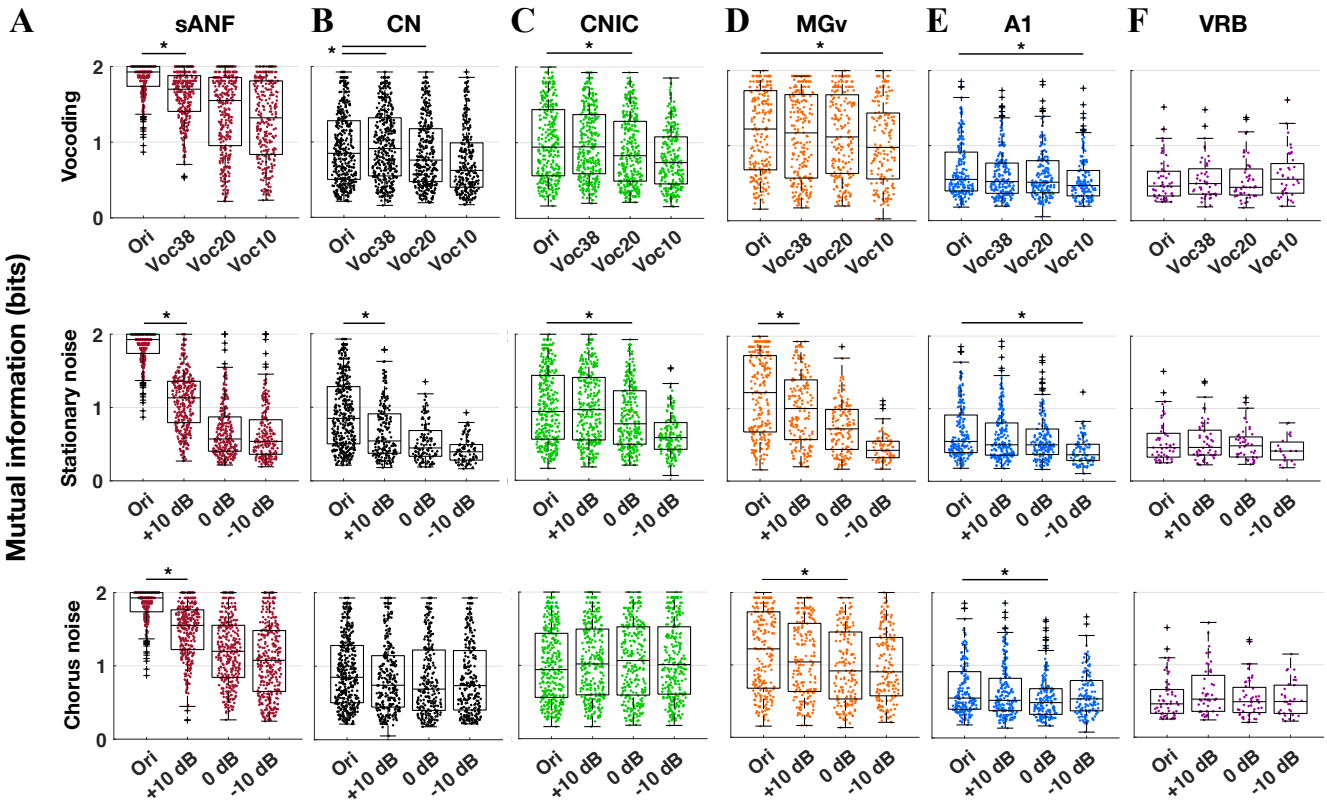
A
sANF
B
CN
C
CNIC
D
MGv
E
A1
F
VRB
Mutual information (bits)
Vocoding
Stationary noise
Chorus noise
0
1
2
*
Ori
Voc38
Voc20
Voc10
+10 dB
0 dB
-10 dB

Figure 4.

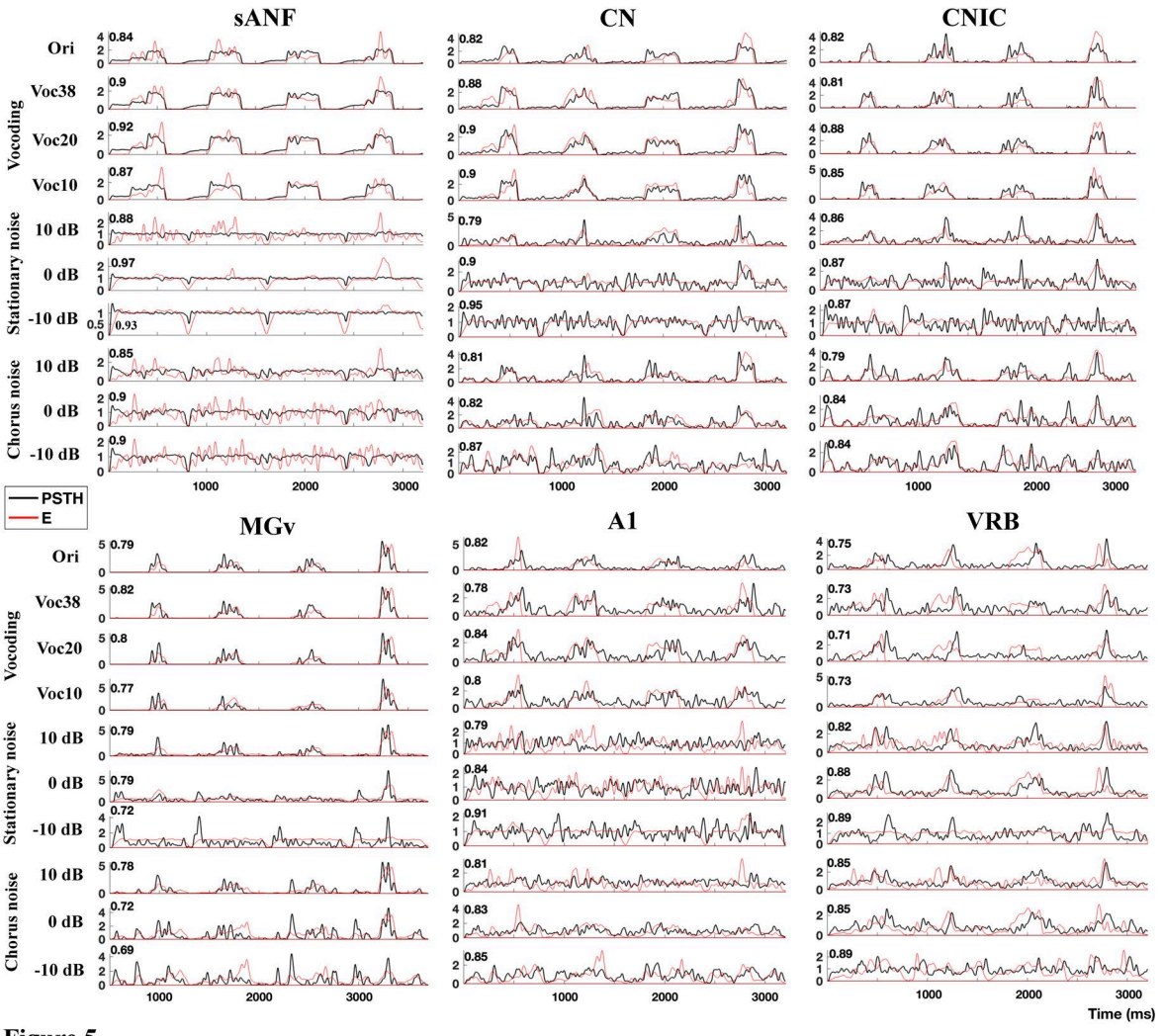
sANF
CN
CNIC
MGv
A1
VRB
Ori
Voc38
Voc20
Voc10
10 dB
0 dB
-10 dB
Vocoding
Stationary noise
Chorus noise
PSTH
E
Time (ms)

Figure 5.

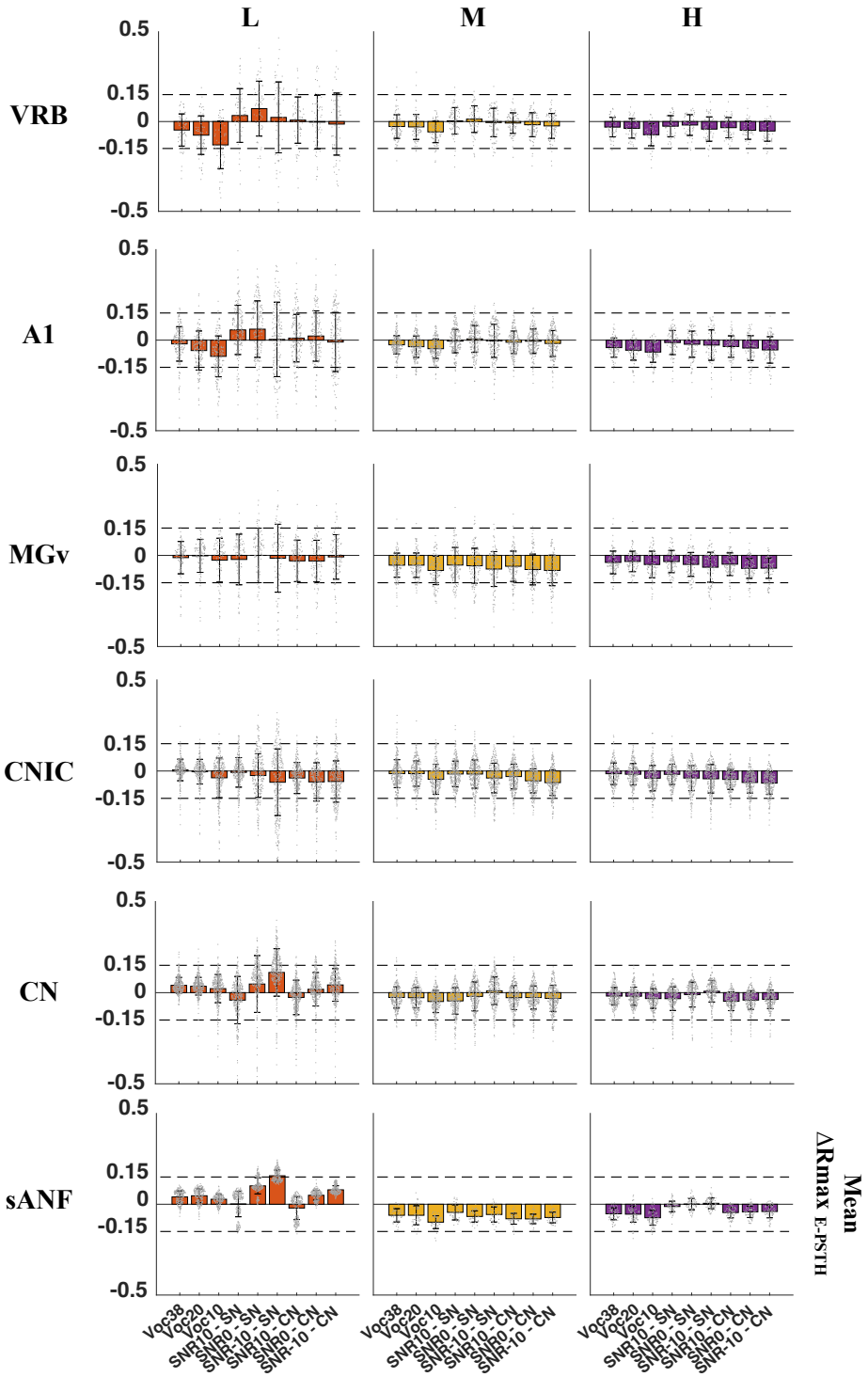
L
M
H
VRB
A1
MGv
CNIC
CN
sANF
0.5
0.15
0
-0.15
-0.5
Voc38
Voc20
Voc10
SNR10 - SN
SNR0 - SN
SNR-10 - SN
SNR10 - CN
SNR0 - CN
SNR-10 - CN
Mean
ΔRmax E-PSTH

Figure 6.

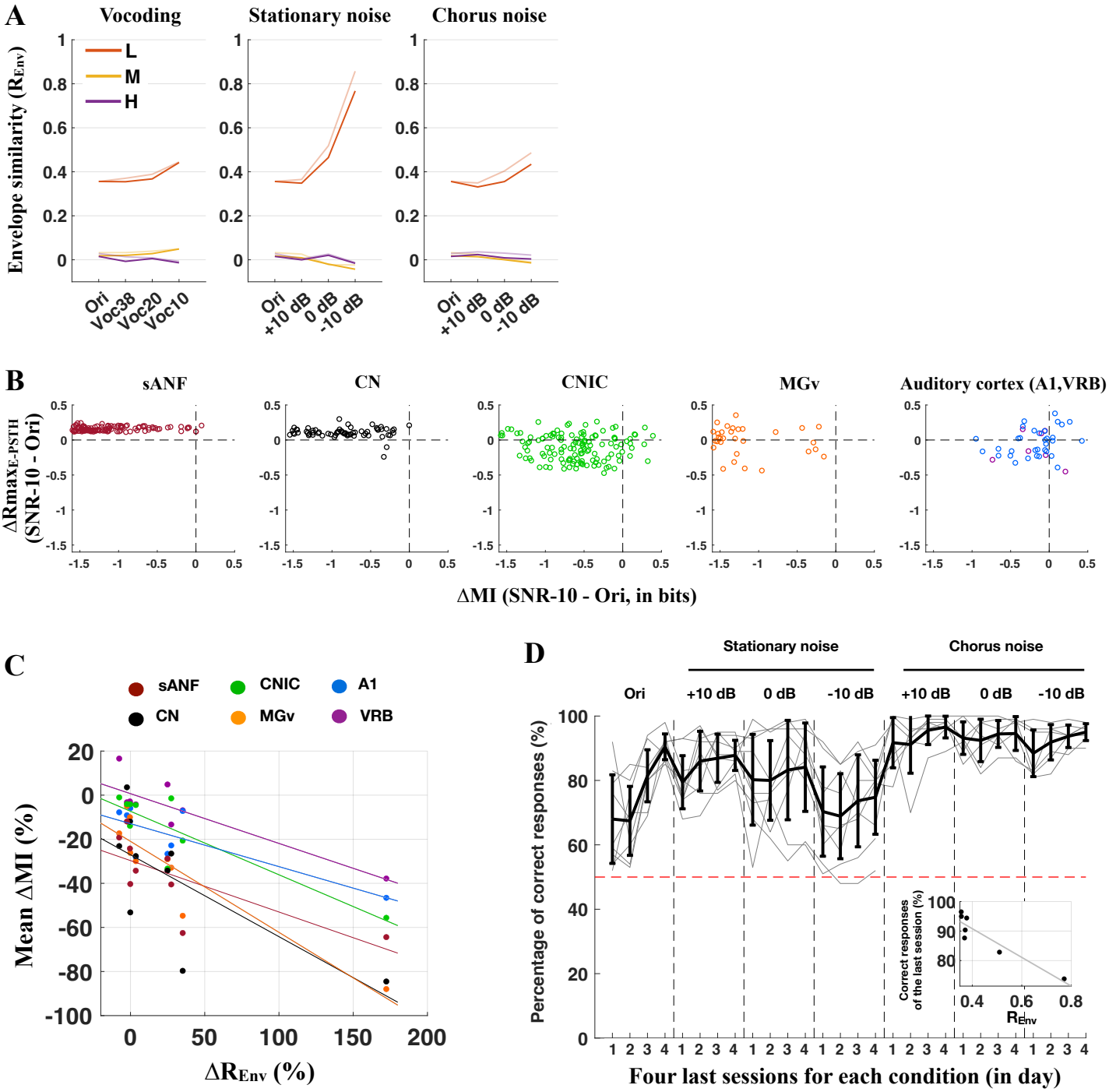
A
Vocoding
Stationary noise
Chorus noise
Envelope similarity (REnv)
L
M
H
Ori
Voc38
Voc20
Voc10
+10 dB
0 dB
-10 dB
B
sANF
CN
CNIC
MGv
Auditory cortex (A1,VRB)
ΔRmaxE-PSTH (SNR-10 - Ori)
ΔMI (SNR-10 - Ori, in bits)
C
sANF
CN
CNIC
MGv
A1
VRB
Mean ΔMI (%)
ΔREnv (%)
D
Stationary noise
Chorus noise
Ori
+10 dB
0 dB
-10 dB
Percentage of correct responses (%)
Correct responses of the last session (%)
REnv
Four last sessions for each condition (in day)

Figure 7.

Methods

Vocalizations in noise

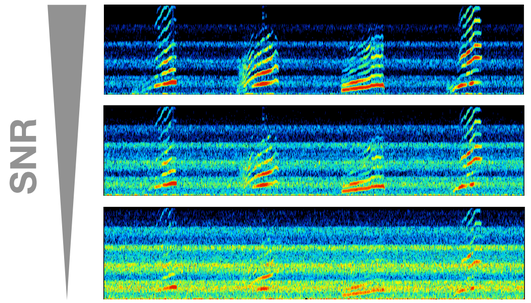

Extracellular recordings from the whole auditory system

+

Simulations of auditory nerve fibers

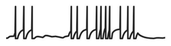

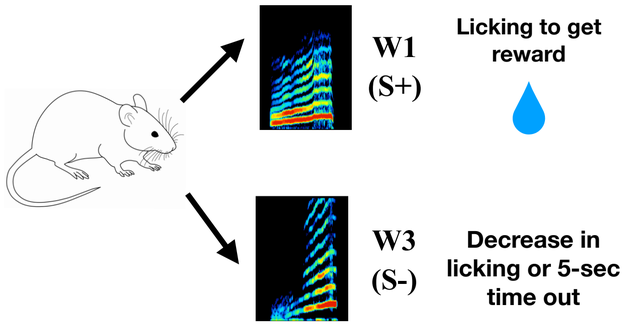

Go/No-Go sound discrimination task

Results

In quiet

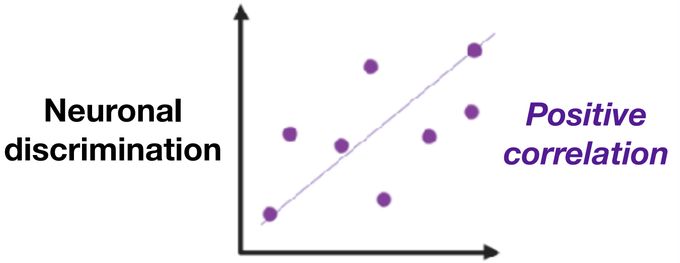

Noise addition

Envelope tracking abilities remain stable